Accepted Manuscript

Design, synthesis and biological evaluation of pyrazol-furan carboxamide analogues as novel Akt kinase inhibitors

Wenhu Zhan, Lei Xu, Xiaowu Dong, Jun Dong, Yi Xiao, Xiaodong Ma, Ni Qiu, Jia Li, Bo Yang, Yubo Zhou, Yongzhou Hu

PII: S0223-5234(16)30257-4

DOI: 10.1016/j.ejmech.2016.03.074

Reference: EJMECH 8499

To appear in: *European Journal of Medicinal Chemistry*

Received Date: 15 January 2016

Revised Date: 12 March 2016

Accepted Date: 25 March 2016

Please cite this article as: W. Zhan, L. Xu, X. Dong, J. Dong, Y. Xiao, X. Ma, N. Qiu, J. Li, B. Yang, Y. Zhou, Y. Hu, Design, synthesis and biological evaluation of pyrazol-furan carboxamide analogues as novel Akt kinase inhibitors, *European Journal of Medicinal Chemistry* (2016), doi: 10.1016/j.ejmech.2016.03.074.

Graphic abstract:

A series of pyrazol-furan carboxamide analogues featuring more restricted conformation in contrast to GSK2141795 were rationally *designed*, *synthesized* and biologically evaluated.

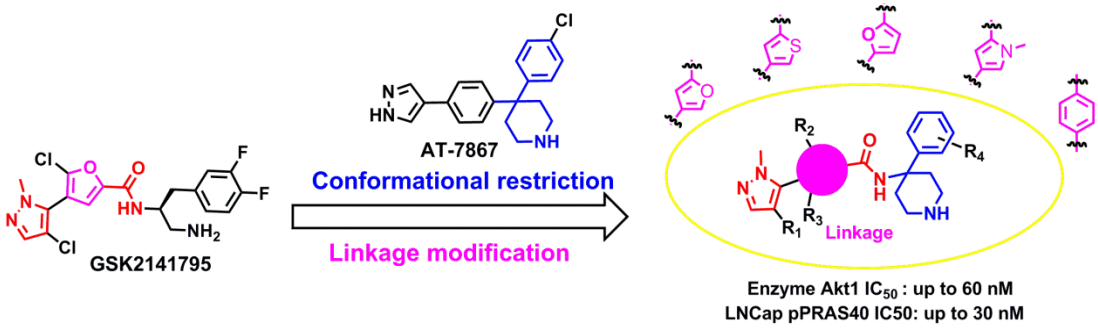

Design, Synthesis and Biological Evaluation of Pyrazol-furan Carboxamide Analogues as Novel Akt Kinase Inhibitors

Wenhu Zhan[a], Lei Xu[b], Xiaowu Dong [a,], Jun Dong[a], Xiao Yi[a], Xiaodong Ma[a], Ni Qiu[a], Jia Li[b], Bo Yang[c], Yubo Zhou[b,]*, Yongzhou Hu[a,]*

[a] *Zhejiang Province Key Laboratory of Anti-Cancer Drug Research, College of Pharmaceutical Sciences, Zhejiang University, Hangzhou, 310058, China*

[b] *National Center for Drug Screening, State Key Laboratory of Drug Research, Shanghai Institute of Materia Medica, Chinese Academy of Sciences, Shanghai 201203, China*

*Corresponding authors:

E-mail: ybzhou@mail.shcnc.ac.cn (Y. Z.); huyz@zju.edu.cn (Y. H.)

Abstract:

A series of novel pyrazol-furan carboxamide analogues were designed, synthesized and biologically evaluated for their Akt1 inhibitory activities, as well as anti-proliferative efficacies against HCT116 and OVCAR-8 cell lines. Most compounds exhibited moderate to excellent Akt1 inhibitory activities, together with favorable cytotoxicities. Further kinase selectivity assay of the most promising compound **25e** illustrated that it was also potent against the structurally related AGC kinases, including Akt2, Akt3, ROCK1 and PKA, but was specific over kinases from other subfamilies. In addition, the Western blot analysis indicated that **25e** could significantly suppress the phosphorylation level of Akt substrate GSK3β in PC-3 cell. Moreover, **25e** demonstrated a concentration-dependent inhibition of phosphorylation of PRAS40 in LNCaP cell, with IC_{50} value of 30.4 nM.

Keywords: Akt1 inhibitor; Synthesis; Cytotoxicity; Molecular docking; Cancer.

1. Introduction

The serine/threonine kinase Akt, also called protein kinase B (PKB), acts as an essential node in the PI3K-Akt-mTOR signaling pathway which plays a critical role in mediating a wide range of cellular functions including survival, metabolism, proliferation, growth and apoptosis [1]. Akt, belonging to the AGC kinase family, is comprised of three highly homologous isoforms in mammals, termed Akt1 (PKB-α), Akt2 (PKB-β) and Akt3 (PKB-γ) [2]. Among them, Akt1 is widely expressed in various tissues, while Akt2 and Akt3 are relatively distinctive, mainly locating in insulin-responsive tissues (Akt2) and brain, lung and kidney (Akt3) [3]. Aberrant activation of Akt has been found in a large number of human cancers, including breast, prostate, lung, ovarian, pancreatic and hematologic malignancies [4-7]. In addition, overexpression of Akt is often associated with poor prognosis and resistance to cancer treatment with chemotherapy or targeted therapies, such as EGFR and BRAF kinase inhibitors [8-10]. Therefore, the inhibition of Akt presents great potential in the treatment of cancers [11-13]. To date, three kinds of Akt inhibitors with different mechanisms of action have been advanced into clinical trial (**Fig. 1**), including phosphatidylinositol analog inhibitors (e.g. Perifosine), allosteric inhibitors (e.g. MK-2206) and ATP-competitive inhibitors (e.g. GDC-0068 and AZD5363) [14-18]. More recently, the structures of novel Akt inhibitors GSK2141795 and GSK2110183 were disclosed, and both of them have entered several advanced clinical trials for the treatment of hematologic and solid malignancies [19-26]. To be of interest, they share the similar skeletons with furan-pyrazole and thiophene-pyrazole moiety respectively, demonstrating that both of these fragments would be promising for Akt1 inhibitors. In this context, with aim to explain the potent Akt1 inhibitory activities, we proposed the possible binding mode between them and the ATP-bound pocket of Akt1 (**Fig. 2A**), consisting of three essential interactions (hinge region, acidic hole and hydrophobic pocket).

As a well-established drug design strategy, the conformational restriction has been frequently introduced to some structurally flexible ligands for optimizing the biological activity, specificity and metabolic stability [27-33]. Considering this, our modification of GSK2141795 prioritized replacing its flexible 3,4-difluorophenylpropanamine with the 4,4-disubstituted-piperidine moiety, a privileged fragment for Akt1 inhibitors bearing more conformational rigidity (e.g. AT-7867) [34, 35]. After assembling this fragment to the furan-pyrazol skeleton, the conformation of the resultant compound **25e** matched favorably to that of GSK2141795 (**Fig. 2B**), thereby testifying its potential as an

alternative to the 3,4-difluorophenylpropanamine. Herein, we reported our continued efforts in the field of Akt inhibitors that culminated in a novel structural series of pyrazol-furan analogues featuring more conformational restriction in contrast to GSK2141795 (**Fig. 3**).

2. Results and discussion

2.1. Chemistry

The synthetic routes for pyrazol-furan carboxamide analogues are outlined in **Scheme 1**-**3**. Suzuki coupling of thiophene-2-carbaldehyde **1** with borate in the presence of $Pd(PPh_3)_4$, afforded pyrazol-thiophene-2-carbaldehyde **2,** which was subsequently converted to **3a**,**b** through electrophilic substitution with NCS or NBS in THF. Oxidation of **2** or **3a**,**b** with $KMnO_4$ in acetone furnished pyrazol-thiophene-2-carboxylic acids **4a-c** in good yields (**Scheme 1**).

The pyrazol-furan-2-carboxylic acid and its analogues were prepared as follows (**Scheme 2**). The bromides **11a**,**b** (Synthetic methods could be found in the *Supporting Information*) were coupled with 1-methyl-5-(4,4,5,5-tetramethyl-1,3,2-dioxaborolan-2-yl)-1H-pyrazole to provide **12a**,**b**. Treatment of compounds **12a**,**b** with different proportions of NCS or NBS at different temperature in THF/DMF, followed by hydrolysis reaction under basic conditions yielded the intermediate **13a-f**. Similarly, key acid fragments **16a-c** and **19a**,**b** could be obtained by using **14** and **17** as the starting materials.

Alkylation of commercially available 2-arylacetonitrile **20a**,**b** with N,N-bis(2-chloroethyl)benzylamine hydrochloride under phase-transfer conditions furnished piperidines **21a**,**b**. Hydrolysis of the cyano group of **21a**,**b** with KOH in 1,2-ethanediol provided acids **22a**,**b**, which subsequently experienced a Curtius rearrangement to give the aminopiperidine derivatives **23a**,**b**. Treatment of **23a**,**b** with **4a-c**, **13a-f**, **16a-c**, or 1**9a**,**b**, followed by removal of the benzyl group yielded the desired compounds **24a-d**, **25a-e**, **26a-c, 27a-c** and **28a**,**b** in excellent yields (**Scheme 3**).

2.2. Akt1 inhibitory and anti-proliferative activities

The Akt1 inhibitory activities of all the target compounds **24a-d**, **25a-e**, **26a-c, 27a-c** and **28a**,**b** were evaluated via a competitive fluorescence polarization kinase activity assay. AZD5363 and GSK2141795, two promising pan-Akt inhibitors under clinical trial, were used as the positive control. The results are summarized in **Table 1**.

As shown in **Table 1**, most of the tested compounds demonstrated moderate to excellent Akt1 inhibitory activities with IC_{50} values ranging from low micromolar to nanomolar level, except for the compounds **26a**, **26c** and **27b** (＜50% inhibition at 1 μg/mL). In the series of thiophen ring as the linker (**24a-d**), introduction of halogen (chloro or bromo) to the 4-position of the pyrazol hinge-binder improved the potency, as exemplified by compounds **24b** and **24c**, which were about 3-fold more potent than **24a**. Replacement of 4-F substitution pattern with 3,4-dichloro on terminal phenyl ring (**24d**, Akt1 IC_{50} = 0.071 μM) resulted in an over 10-fold improvement in Akt1 potency, which is consistent with the SAR of previously reported Akt inhibitors [36]. In the set of furan-linked analogues **25a-e**, most of the compounds showed similar Akt1 inhibitory effect to that of **24a-d**. Introduction of a chlorine substituent at the 5-position of furan linkage boosted the potency (**25d** vs **25a**). Further introduction of 3,4-dichloro substitution pattern into **25d** gave **25e,** the direct analogue of GSK2141795**,** which was proved to be most potent throughout the series (IC_{50} = 0.061 μM) and pertained to the same order of magnitude as AZD5363 (IC_{50} = 0.034 μM) and GSK2141795 (IC_{50} = 0.018 μM). Translocation of pyrazol moieties to 5-position of furyl linkage gave **26a-c**. Unfortunately, this modification was proved to be detrimental to the inhibitory potency. Encouraged by this, we subsequently probed SARs around a selection of linkages. N-methylpyrrol analogues **27a-c**, showed somewhat reduced Akt1 inhibiting effect. In addition, a larger phenyl linkage was also found to be of no benefit to Akt1inhibitory potency, as illustrated by compounds **28a**,**b**.

Furthermore, all the above compounds were tested for their anti-proliferative activities *in vitro* against two human cancer cell lines including OVCAR-8 (Ovarian Adenocarcinoma) and HCT116 (Human Colon Cancer) by Sulforhodamine B (SRB) assay. All of them exhibited moderate to potent cytotoxicities against both cell lines as outlined in **Table 1**. Among them, **24d** bearing a 2,4-disubstituted thiophen linker was the most remarkable with IC_{50} values of 1.61 μM and 3.92 μM against OVCAR-8 and HCT-116 cell lines, respectively. It is noteworthy that compound **25e**, the most potent Akt1 inhibitor (Akt1 IC_{50} = 0.061 μM)) of this series, also displayed favorable anti-proliferative activities against OVCAR-8 (IC_{50} = 9.76 μM) and HCT-116 (IC_{50} = 7.76 μM) cell lines, which was comparable to AZD5363 with the IC_{50} values of 7.27 and 5.20 μM, respectively.

2.3. Kinase selectivity assay

In order to investigate the selectivity profile of target compounds, compound **25e** was evaluated

against a panel of over 20 kinases at concentrations of 10 μM and 0.5 μM.

According to the biological data in **Table 2**, **25e** exhibited favorable specificity over kinases form subfamilies including TK, CAMK, TKL, CMGC. However, as for other two Akt isoforms or kinases highly homologous to Akt1 in the AGC family, the selectivity was compromised to some extent. At the 0.5μM, more than 50% inhibition was obtained against PKA, RSK1, P70S6K, ROCK1, SGK, MSK1 and PRKG1.

2.4. Western blot analysis

Compound **25e** was further assessed for its capability to downregulate the phosphorylation of GSK3β (S9), a key downstream effector of Akt in PC-3 cell line using Western Blot assay. As illustrated in **Fig. 4**, **25e** exhibited a significant inhibition effect on the phosphorylated GSK3β (S9), without decreasing the overall total GSK3β, Akt and GAPDH protein levels. In addition, a feedback increase in phosphorylated Akt (S473) was observed at 1μM, whereas phosphorylation on Akt was also inhibited at higher concentration (10 μM). This phenomenon was consistent with that observed for a myriad of ATP-competitive Akt inhibitors [37-39].

2.5. Phosphorylated PRAS40 (pThr246) cellular ELISA assay

Subsequently, the IC_{50} value against Akt was determined for **25e** at the cellular level *via* ELISA assay. The PTEN-null LNCaP prostate cell line was used for this analysis due to its overactive Akt pathway. As shown in **Fig. 5**, **25e** demonstrated a pronounced effect on the inhibition of phosphorylation of PRAS40, a known Akt substrate, with IC_{50} value of 30.4 nM, which was over 10- and 2-fold more efficacious than AZD5363 and GSK2141795, respectively.

2.6. Molecular docking study

With an attempt to explore the possible binding modes of these pyrazol-furan analogues, **25e** and **28a** were docked into the Akt1 catalytic cleft on the basis of the co-crystal structure of AZD5363 complexed with Akt1.

As shown in **Fig. 6A**, compound ***25e*** occupied the ATP binding site of Akt1 via conferring four hydrogen bonds. Firstly, the pyrazol ring formed an essential hydrogen bond with residue Ala230. Meanwhile, the hydrogen of amide attached to the furan linkage served as an H-bond donor for

Asp292. Besides, the basic piperidine group interacted with the side chains of Asn279 and Glu278 in the carbonyl-rich region *via* two hydrogen bonds. Beyond these H-bond interaction, the 3,4-dichlorophenyl group of **25e** inserted into a small hydrophobic pocket under the P-loop and generated substantial hydrophobic contacts with neighboring residues, thereby accounting for its favorable binding affinity. As for **28a**, however, the larger phenyl linkage had to move away from the neighboring residue for obviating the unfavorable contact. Consequently, the H-bond interactions of the piperidine group with Asn279 and Glu278 decreased due to the concerted movement of the whole molecule, hence weakening the potency.

3. Conclusion

On the basis of the structures of GSK2141795, we rationally designed and synthesized a series of pyrazol-furan carboxamide analogues featuring more restricted conformation. Most of them exhibited moderate to excellent Akt1 inhibitory activities, as well as preferable anti-proliferative efficacy against HCT116 and OVCAR-8 cell lines. Besides, kinase selectivity assay of the representative **25e** illustrated that it is also potent against the several structurally related AGC kinases, but was specific over kinases from other subfamilies. In addition, Western blot analysis indicated that **25e** could markedly suppress the phosphorylation level of Akt substrate GSK3β in PC-3 cell. Moreover, **25e** significantly decreased the level of p-PRAS40 with IC_{50} value of 30.4 nM in LNCAP cell, which is much more efficient than AZD5363. Finally, the binding mode between AKT1 with compound **25e** was proposed by molecular docking. In conclusion, compound **25e** was identified as a potent pan-Akt inhibitor with vigorous cellular activity, which merited further development as a potential anticancer agent.

4. Experimental

4.1. Chemistry

Melting points were obtained on a B-540 Büchi melting-point apparatus and are uncorrected. ^{1}H NMR spectra were recorded on a 500 MHz, ^{13}C NMR were recorded on a 125 MHz spectrometer, respectively (chemical shifts are given in ppm (δ) relative to TMS as internal standard, coupling constants (J) are in hertz (Hz), and signals are designated as follows: s, singlet; d, doublet; t, triplet; m, multiplet; br s, broad singlet, etc.). Mass spectral data were obtained on an Esquire-LC-00075

spectrometer. High resolution mass spectra were measured on an Agilent 1290 HPLC-6224 Time of Fight Mass Spectrometer.

*4.1.1 4-(1-Methyl-1H-pyrazol-5-yl)thiophene-2-carbaldehyde **2***

To a solution of 4-bromothiophene-2-carbaldehyde **1** (3.82 g, 20 mmol) in 1,4-dioxane/H_2O (v/v = 3/1, 60 mL) was added K_2CO_3 (5.52 g, 40 mmol) and 1-methyl-5-(4,4,5,5-tetramethyl-1,3,2-dioxaborolan-2-yl)-1H-pyrazole (5.0 g, 24 mmol), followed by tetrakistriphenylphosphane Pd (0) (1.16 g, 5 mol %). The reaction mixture was heated at reflux under nitrogen for 6 h. After cooling to r.t., the reaction solution was poured into H_2O (50 mL) and extracted with ethyl acetate (15 mL × 3). The combined organic layers were dried over Na_2SO_4, concentrated under vacuum and purified on silica gel to afford the title compound **2** as a pale yellow solid (3.11 g, 81%), mp: 70-72 °C.

^{1}H NMR (500 MHz, $CDCl_3$) δ 9.98 (d, *J* = 1.1 Hz, 1H), 7.85 (d, *J* = 1.1 Hz, 1H), 7.77 (s, 1H), 7.53 (d, *J* = 1.9 Hz, 1H), 6.39 (d, *J* = 1.9 Hz, 1H), 3.97 (s, 3H). ESI-MS: m/z = 193 $[M + 1]^+$.

*4.1.2 General procedure for preparation of compound **3a** and **3b***

A mixture of **2** (960 mg, 5 mmol) and NCS or NBS in dry THF (15 mL) was stirred at r.t. for 3 h. The reaction mixture was concentrated and the crude residue was extracted with ethyl acetate and washed with saturated aqueous Na_2CO_3. The organic layer was further washed with brine, dried over anhydrous Na_2SO_4, and then concentrated, recrystallized from ethyl acetate to give the title compound.

*4.1.2.1 4-(4-Chloro-1-methyl-1H-pyrazol-5-yl)thiophene-2-carbaldehyde **3a***

Reagent: NCS (798 mg, 6 mmol). The product was obtained as an off-white solid (1.0 g, 90%), mp: 98-100 °C. ^{1}H NMR (500 MHz, $CDCl_3$) δ 10.01 (d, *J* = 1.1 Hz, 1H), 7.92 (d, *J* = 1.1 Hz, 1H), 7.90 (s, 1H), 7.52 (s, 1H), 3.91 (s, 3H). ESI-MS (*m/z*): 227 $[M + 1]^+$.

*4.1.2.2 4-(4-Bromo-1-methyl-1H-pyrazol-5-yl)thiophene-2-carbaldehyde **3b***

Reagent: NBS (980 mg, 5.5 mmol). The product was obtained as a yellow solid (1.23 g, 92%), mp: 92-95 °C. ^{1}H NMR (500 MHz, $CDCl_3$) δ 10.00 (s, 1H), 7.91 (s, 1H), 7.90 (s, 1H), 7.54 (s, 1H), 3.90 (s, 3H). ESI-MS (*m/z*): 271 $[M + 1]^+$.

*5.1.3 General procedure for synthesis of compounds **4a-4c***

To a solution of aldehyde in acetone (30 mL) at 0 °C was added potassium permanganate (380 mg, 2.4mmol) in one portion. The mixture was stirred at r.t. for 3 h, then the potassium salts were filtered

off and the filtrate was concentrated and purified on silica gel to give the title compounds.

*4.1.3.1 4-(1-Methyl-1H-pyrazol-5-yl)thiophene-2-carboxylic acid **4a***

Reagent: **2** (385 mg, 2 mmol). The product was obtained as a white solid (345 mg, 83%). ^{1}H NMR (500 MHz, DMSO) δ 13.27 (s, 1H), 8.10 (d, *J*=1.4 Hz, 1H), 7.93 (d, *J*=1.4 Hz, 1H), 7.43 (d, *J*=1.8 Hz, 1H), 6.54 (d, *J*=1.8 Hz, 1H), 3.92 (s, 3H). ESI-MS (*m/z*): 207 $[M - H]^-$.

*4.1.3.2 4-(4-Chloro-1-methyl-1H-pyrazol-5-yl)thiophene-2-carboxylic acid **4b***

Reagent: **3a** (452 mg, 2 mmol). The product was obtained as a white solid (411 mg, 85%). ^{1}H NMR (500 MHz, DMSO) δ 13.35 (s, 1H), 8.20 (d, *J* = 1.5 Hz, 1H), 7.93 (d, *J* = 1.5 Hz, 1H), 7.64 (s, 1H), 3.84 (s, 3H). ESI-MS (*m/z*): 241 $[M - H]^-$.

*4.1.3.3 4-(4-Bromo-1-methyl-1H-pyrazol-5-yl)thiophene-2-carboxylic acid **4c***

Reagent: **3b** (540 mg, 2 mmol). The product was obtained as a white solid (510 mg, 89%). ^{1}H NMR (500 MHz, DMSO) δ 13.37 (s, 1H), 8.19 (d, *J* =1.5Hz, 1H), 7.92 (d, *J* =1.5Hz, 1H), 7.64 (s, 1H), 3.84 (s, 3H). ESI-MS (*m/z*): 285 $[M - H]^-$.

*4.1.4 General procedure of Suzuki coupling for compounds **12a**, **12b**, **15** and **18***

Tetrakistriphenylphosphane Pd (0) (580 mg, 5 mol %) was added to a stirred suspension of 1-methyl-5-(4,4,5,5-tetramethyl-1,3,2-dioxaborolan-2-yl)-1H-pyrazole (2.5 g, 12 mmol), $K_3PO_4 \cdot 3H_2O$ (4.8 g, 18 mmol) and the corresponding bromide in DMF (100 mL) at 0 °C under nitrogen. The reaction mixture was heated at 80-120 °C for 8 h, then poured into H_2O (100 mL) and extracted with ethyl acetate (45 mL × 3). The combined organic layers were washed with brine (50 mL × 2), dried over Na_2SO_4, and concentrated under vacuum to afford an off-white semisolid. The crude product was purified by flash silica chromatography to obtain the title compound.

*4.1.4.1 Methyl 4-(1-methyl-1H-pyrazol-5-yl)furan-2-carboxylate **12a***

Reagent: methyl 4-bromofuran-2-carboxylate **11a** (2.05 g, 10 mmol, *Supporting Information*). The product was obtained as a white solid (1.63 g, 79%). ^{1}H NMR (500 MHz, $CDCl_3$) δ 7.73 (d, *J* = 0.8 Hz, 1H), 7.48 (d, *J* = 1.9 Hz, 1H), 7.31 (d, *J* = 0.8 Hz, 1H), 6.34 (d, *J* = 1.9 Hz, 1H), 3.94 (s, 3H), 3.93 (s, 3H). ESI-MS (*m/z*): 207 $[M + 1]^+$.

*4.1.4.2 Methyl 1-methyl-4-(1-methyl-1H-pyrazol-5-yl)-1H-pyrrole-2-carboxylate **12b***

Reagent: methyl 4-bromo-1-methyl-1H-pyrrole-2-carboxylate **11b** (2.18 g, 10 mmol, *Supporting Information*). The product was obtained as a white solid (1.49 g, 68%).^{1}H NMR (500 MHz, $CDCl_3$) δ 7.45 (d, *J* = 1.8 Hz, 1H), 7.04 (d, *J* = 2.0 Hz, 1H), 6.94 (d, *J* = 2.0 Hz, 1H), 6.23 (d, *J* = 1.8 Hz, 1H),

3.98 (s, 3H), 3.94 (s, 3H), 3.85 (s, 3H). ESI-MS (*m/z*): 220 $[M + 1]^+$.

*4.1.4.3 Methyl 4-bromo-5-(1-methyl-1H-pyrazol-5-yl)furan-2-carboxylate **15***

Reagent: methyl 4,5-dibromofuran-2-carboxylate **14** (2.84 g, 10 mmol). The product was obtained as a white solid (2.36 g, 83%). ^{1}H NMR (500 MHz, $CDCl_3$) δ 7.54 (d, *J* = 2.1 Hz, 1H), 7.29 (s, 1H), 6.92 (d, *J* = 2.1 Hz, 1H), 4.14 (s, 3H), 3.92 (s, 3H). ESI-MS (*m/z*): 285 $[M + 1]^+$.

*4.1.4.4 Methyl 4-(1-methyl-1H-pyrazol-5-yl)benzoate **18***

Reagent: methyl 4-bromobenzoate **17** (2.15 g, 10 mmol). The product was obtained as a white solid (2.05 g, 95%). ^{1}H NMR (500 MHz, $CDCl_3$) δ 8.12 (d, *J* = 8.3 Hz, 2H), 7.54 (d, *J* = 1.9 Hz, 1H), 7.51 (d, *J* = 8.3 Hz, 2H), 6.38 (d, *J* = 1.9 Hz, 1H), 3.95 (s, 3H), 3.93 (s, 3H). ESI-MS (*m/z*): 217 $[M + 1]^+$.

*4.1.5 General procedure for preparation of compounds **13a-f, 16a-c, 19a** and **19b***

To a solution of the above methyl carboxylate (5 mmol) in dry THF/DMF at 0 °C was added NCS or NBS (6−20 mmol) in one portion. The reaction mixture was stirred at r.t.−80 °C for 0.5–6 h, then was diluted with ethyl acetate and washed with saturated aqueous $NaHCO_3$. The organic layer was further washed well with brine, concentrated under vacuum to afford the halogenated product, which was subsequently dissolved in THF, and sodium hydroxide aqueous solution (2 N, 10 mL) was added. The mixture was allowed to stir at r.t. for 3–10 h, then the solvent was removed and the resulting crude mixture was dissolved in 20 mL of water and acidified with concentrated hydrochloric acid until pH 1, and extracted with ethyl acetate (10 mL × 3), the combined organic layers was further washed with brine, dried over anhydrous Na_2SO_4, and then concentrated to dryness to yield the title acid.

*4.1.5.1 4-(4-Chloro-1-methyl-1H-pyrazol-5-yl)furan-2-carboxylic acid **13a***

Reagent: **12a** (1.03 g, 5 mmol) and NCS (800 mg, 6 mmol), r.t., THF (15 mL). The product was obtained as a white solid (788 mg, 70%). ^{1}H NMR (500 MHz, DMSO) δ 13.48 (s, 1H), 8.38 (s, 1H), 7.64 (s, 1H), 7.58 (s, 1H), 3.87 (s, 3H). ESI-MS (*m/z*): 225 $[M - H]^-$.

*4.1.5.2 5-Chloro-4-(4-chloro-1-methyl-1H-pyrazol-5-yl)furan-2-carboxylic acid **13b***

Reagent: **12a** (1.03 g, 5 mmol) and NCS (2.67 g, 20 mmol), 80 °C, THF/DMF (v/v = 1/1, 20 mL). The product was obtained as a white solid (820 mg, 63%). ^{1}H NMR (500 MHz, DMSO) δ 13.75 (s, 1H), 7.70 (s, 1H), 7.69 (s, 1H), 3.77 (s, 3H). ESI-MS (*m/z*): 259 $[M - H]^-$.

*4.1.5.3 4-(4-Bromo-1-methyl-1H-pyrazol-5-yl)furan-2-carboxylic acid **13c***

Reagent: **12a** (1.03 g, 5 mmol) and NBS (1.07 g, 6 mmol), r.t., THF (15 mL). The product was obtained as a white solid (1.11 g, 82%). ^{1}H NMR (500 MHz, DMSO) δ 12.16 (s, 1H), 8.36 (s, 1H), 7.65 (s, 1H), 7.58 (s, 1H), 3.87 (s, 3H). ESI-MS (*m/z*): 269 [M − H]$^-$.

4.1.5.4 4-(4-Bromo-1-methyl-1H-pyrazol-5-yl)-1-methyl-1H-pyrrole-2-carboxylic acid ***13d***

Reagent: **12b** (1.10 g, 5 mmol) and NBS (908 mg, 5.1 mmol), r.t., THF (15 mL). The product was obtained as an off-white solid (1.03 g, 73%). ^{1}H NMR (500 MHz, $CDCl_3$) δ 7.51 (s, 1H), 7.24 (d, *J* = 1.6 Hz, 1H), 7.17 (d, *J* = 1.6 Hz, 1H), 4.02 (s, 3H), 3.92 (s, 3H). ESI-MS (*m/z*): 282 [M − H]$^-$.

4.1.5.5 5-Bromo-4-(4-bromo-1-methyl-1H-pyrazol-5-yl)-1-methyl-1H-pyrrole-2-carb- oxylic acid ***13e***

Reagent: **12b** (1.10 g, 5 mmol) and NBS (1.96 g, 11 mmol), 40 °C, THF (20 mL). The product was obtained as an off-white solid (1.21 g, 67%). ^{1}H NMR (500 MHz, $CDCl_3$) δ 7.57 (s, 1H), 7.19 (s, 1H), 4.05 (s, 3H), 3.78 (s, 3H). ESI-MS (*m/z*): 362 [M − H]$^-$.

4.1.5.6 3,5-Dichloro-4-(4-chloro-1-methyl-1H-pyrazol-5-yl)-1-methyl-1H-pyrrole-2- carboxylic acid ***13f***

Reagent: **12b** (1.10 g, 5 mmol) and NCS (2.13 g, 16 mmol), 70 °C, THF/DMF (v/v = 2/1, 20 mL). The product was obtained as an off-white solid (982 mg, 64%). ^{1}H NMR (500 MHz, DMSO) δ 12.92 (s, 1H), 7.70 (s, 1H), 3.92 (s, 3H), 3.67 (s, 3H). ESI-MS (*m/z*): 306 [M − H]$^-$.

4.1.5.7 4-Bromo-5-(1-methyl-1H-pyrazol-5-yl)furan-2-carboxylic acid ***16a***

Reagent: **15** (1.42 g, 5 mmol), treated with sodium hydroxide aqueous solution directly. The product was obtained as a white solid (1.28 g, 95%). ^{1}H NMR (500 MHz, $CDCl_3$) δ 7.54 (d, *J* = 2.3 Hz, 1H), 7.41 (s, 1H), 6.97 (s, 1H), 6.68 (d, *J* = 2.3 Hz, 1H), 4.17 (s, 3H). ESI-MS (*m/z*): 269 [M − H]$^-$.

4.1.5.8 4-Bromo-5-(4-chloro-1-methyl-1H-pyrazol-5-yl)furan-2-carboxylic acid ***16b***

Reagent: **15** (1.42 g, 5 mmol), and NCS (800 mg, 6 mmol), r.t., THF (15 mL). The product was obtained as a white solid (1.35 g, 89%). ^{1}H NMR (500 MHz, $CDCl_3$) δ 7.55 (s, 1H), 7.45 (s, 1H), 3.89 (s, 3H). ESI-MS (*m/z*): 305 [M − H]$^-$.

4.1.5.9 4-Bromo-5-(4-bromo-1-methyl-1H-pyrazol-5-yl)furan-2-carboxylic acid ***16c***

Reagent: **15** (1.42 g, 5 mmol), and NBS (908 mg, 5.1 mmol), r.t., THF (15 mL). The product was obtained as a white solid (1.53 g, 88%). ^{1}H NMR (500 MHz, $CDCl_3$) δ 7.59 (s, 1H), 7.46 (s, 1H), 3.90 (s, 3H). ESI-MS (*m/z*): 349 [M − H]$^-$.

*4.1.5.10 4-(4-Chloro-1-methyl-1H-pyrazol-5-yl)benzoic acid **19a***

Reagent: **18** (1.08 g, 5 mmol), and NCS (800 mg, 6 mmol), r.t., THF (15 mL). The product was obtained as a white solid (1.07 g, 91%). 1H NMR (500 MHz, DMSO) δ 8.11 – 8.08 (m, 2H), 7.70 (s, 1H), 7.68 – 7.64 (m, 2H), 3.80 (s, 3H). ESI-MS (*m/z*): 235 $[M - H]^-$.

*4.1.5.11 4-(4-Bromo-1-methyl-1H-pyrazol-5-yl)benzoic acid **19b***

Reagent: **18** (1.08 g, 5 mmol), and NBS (908 mg, 5.1 mmol), r.t., THF (15 mL). The product was obtained as a white solid (1.17 g, 84%). ^{1}H NMR (500 MHz, $CDCl_3$) δ 8.26 (d, *J* = 8.3 Hz, 2H), 7.59 (s, 1H), 7.56 (d, *J* = 8.3 Hz, 2H), 3.87 (s, 3H). ESI-MS (*m/z*): 279 $[M - H]^-$.

*4.1.6 General procedure for preparation of compound **21a** and **21b***

To a well stirred suspension of tetrabutylammonium hydrogen sulfate (0.34 g, 1 mmol), N,N-Bis(2-chloroethyl)benzylamine hydrochloride (2.69 g, 10 mmol), and 2-arylacetonitrile in toluene (10 mL) was added dropwise 5 g of 50% (w/w) aqueous NaOH solution. The reaction mixture was heated at 85 °C for 4 h, then poured into ice-water (30 mL) and extracted with ethyl ether (15 mL × 3). The combined organic layers were dried over Na_2SO_4, concentrated under vacuum, and the crude product was purified by flash silica chromatography to obtain the title compound.

*4.1.6.1 1-Benzyl-4-(4-fluorophenyl)piperidine-4-carbonitrile **21a***

Reagent: 2-(4-fluorophenyl)acetonitrile **20a** (1.35g, 10 mmol). The product was obtained as a yellow oil (2.06 g, 70%). ^{1}H NMR (500 MHz, $CDCl_3$) δ 7.51 – 7.44 (m, 2H), 7.34 (m, 4H), 7.28 (m, 1H), 7.11 – 7.05 (m, 2H), 3.61 (s, 2H), 3.01 (d, J = 12.2 Hz, 2H), 2.56 – 2.48 (m, 2H), 2.10 (t, J = 9.5 Hz, 4H). ESI-MS (*m/z*): 295 $[M+1]^+$.

*4.1.6.2 1-Benzyl-4-(3,4-dichlorophenyl)piperidine-4-carbonitrile **21b***

Reagent: 2-(3,4-dichlorophenyl)acetonitrile **20b** (1.85g, 10 mmol). The product was obtained as a yellow oil (2.23 g, 65%). ^{1}H NMR (500 MHz, $CDCl_3$) δ 7.59 (d, *J* = 2.3 Hz, 1H), 7.48 – 7.46 (m, 1H), 7.37 – 7.32 (m, 5H), 7.31 – 7.26 (m, 1H), 3.60 (s, 2H), 3.01 (d, *J* = 12.5 Hz, 2H), 2.56 – 2.42 (m, 2H), 2.09 – 2.05 (m, 4H). ESI-MS (*m/z*): 345 $[M+1]^+$.

*4.1.7 General procedure for preparation of compound **22a** and **22b***

To a suspension of **21** in 1,2-ethanediol (20 mL) was add KOH (5.6g, 100 mmol), and the mixture was allowed to stir at 180°C for 20 h. After cooling to room temperature, the solution was poured into ice-water (100 mL), and washed with ethyl ether (50 mL × 2), then acidified with concentrated

hydrochloric acid until pH 5. The precipitate was filtrated, rinsed with cooled ethyl ether and dried to afford the title compound.

*4.1.7.1 1-Benzyl-4-(4-fluorophenyl)piperidine-4-carboxylic acid **22a***

Reagent: **21a** (2.95g, 10 mmol). ^{1}H NMR (500 MHz, DMSO) δ 7.41 (dd, *J* = 8.9, 5.4 Hz, 2H), 7.34 – 7.26 (m, 4H), 7.24 (dd, *J* = 10.7, 4.2 Hz, 1H), 7.16 (t, *J* = 8.9 Hz, 2H), 3.44 (s, 2H), 2.70 (d, *J* = 9.6 Hz, 2H), 2.40 (d, *J* = 12.8 Hz, 2H), 2.14 (t, *J* = 10.9 Hz, 2H), 1.78 (t, *J* = 10.6 Hz, 2H). The product was obtained as a white solid (2.23 g, 71%). ESI-MS (*m/z*): 314 $[M+1]^+$.

*4.1.7.2 1-Benzyl-4-(3,4-dichlorophenyl)piperidine-4-carboxylic acid **22b***

Reagent: **21b** (3.44g, 10 mmol). The product was obtained as an off-white solid (2.72 g, 75%). ^{1}H NMR (500 MHz, $CDCl_3$) δ 7.59 (d, *J* = 2.3 Hz, 1H), 7.48 – 7.45 (m, 1H), 7.38 – 7.31 (m, 5H), 7.31 – 7.25 (m, 1H), 3.60 (s, 2H), 3.01 (m , 2H), 2.57 – 2.45 (m, 2H), 2.11 – 2.05 (m, 4H). ESI-MS (*m/z*): 364 $[M+1]^+$.

*4.1.8 General procedure for preparation of compounds **23a**,**b***

To a solution of **22** in anhydrous toluene (15 mL) was added triethylamine (0.28 mL, 2.0 mmol), followed by the addition of diphenyl phosphoryl azide (0.32 mL, 1.5 mmol). The mixture was stirred at room temperature under nitrogen for 1 hour and then heated at 90 °C for 3 h. After cooling down to room temperature, the solution was poured into a hydrochloric aqueous solution (6 N, 20 mL), and the resulting mixture was heated at reflux for 3h. The solvent was concentrated and the residue was dissolved in a saturated solution of $NaHCO_3$ in water (20 mL), and extracted with ethyl acetate (10 mL × 3). The combined organic layers were dried over Na_2SO_4, concentrated under vacuum and purified on silica gel to afford the title amine.

*4.1.8.1 1-Benzyl-4-(4-fluorophenyl)piperidin-4-amine **23a***

Reagent: **22a** (313 mg, 1.0 mmol). The product was obtained as a yellow solid (207 mg, 73%). ^{1}H NMR (500 MHz, DMSO) δ 7.58 – 7.53 (m, 2H), 7.30 (dd, *J* = 8.7, 4.2 Hz, 4H), 7.23 (dt, *J* = 5.6, 4.2 Hz, 1H), 7.12 – 7.06 (m, 2H), 3.48 (s, 2H), 3.35 (s, 2H), 2.48 – 2.44 (m, 2H), 1.96 – 1.89 (m, 2H), 1.72 (s, 2H), 1.54 (d, *J* = 12.2 Hz, 2H). ESI-MS (*m/z*): 285 $[M+1]^+$.

*4.1.8.2 1-Benzyl-4-(3,4-dichlorophenyl)piperidin-4-amine **23b***

Reagent: **22b** (364 mg, 1.0 mmol). The product was obtained as a pale yellow solid (227 mg, 68%). ESI-MS (*m/z*): 335 $[M+1]^+$.

*4.1.9 General procedure for synthesis of the target compounds **24a-d**, **25a-e, 26a-c, 27a-c**, and*

28a*,*b.

To a solution of carboxylic acid, 1-(3-dimethylaminopropyl)-3-ethylcarbodiimide hydrochloride (77 mg, 0.4 mmol) and 1-hydroxybenzotriazole (54 mg, 0.4 mmol) in DCM (5 mL) at 0 °C was added triethylamine (0.11 mL, 0.6 mmol), followed by the addition of corresponding amine. The mixture was stirred at r.t. overnight, and then partitioned between ethyl acetate (20 mL) and brine (15 mL × 3). The organics were dried over Na_2SO_4, concentrated under vacuum. The resulting white solid was dissolved in 1,2-dichloroethane (5 mL) and 1-chloroethyl chloroformate (43 mg, 0.3 mmol) was added. The resulting mixture was stirred at r.t. for 3 h, evaporated in vacuo, and then treated with methanol (3 mL) at reflux for 1 h. After cooling to r.t., the mixture was basified with saturated aqueous $NaHCO_3$ (10 mL) and extracted with ethyl acetate (5 mL × 3). The combined organic layers was further washed well with brine, dried over Na_2SO_4, concentrated under vacuum and purified on silica gel to afford the title compound.

4.1.9.1 N-(4-(4-fluorophenyl)piperidin-4-yl)-4-(1-methyl-1H-pyrazol-5-yl)thiophene-2-carboxamide ***24a***

Reagent: **4a** (42 mg, 0.2 mmol) and **23a** (57 mg, 0.2 mmol). The product was obtained as a white solid (44 mg, 57%), mp: 159-161 °C. ^{1}H NMR (500 MHz, $CDCl_3$) δ 7.64 (s, 1H), 7.49 (d, *J* = 1.6 Hz, 1H), 7.47 (s, 1H), 7.45 – 7.40 (m, 2H), 7.03 (t, J = 8.6 Hz, 2H), 6.35 (d, *J* = 1.6 Hz, 1H), 6.31 (s, 1H), 3.94 (s, 3H), 3.11 – 2.98 (m, 4H), 2.51 (d, *J* = 13.4 Hz, 2H), 2.16 – 2.09 (m, 2H). ESI-MS (*m/z*): 385 $[M+1]^+$. HRMS (ESI): *m/z* calcd for $(C_{20}H_{21}FN_4OS+H)^+$: 385.1493; found: 385.1507.

4.1.9.2

4-(4-Chloro-1-methyl-1H-pyrazol-5-yl)-N-(4-(4-fluorophenyl)piperidin-4-yl)-thiophene-2-carboxamide ***24b***

Reagent: **4b** (49 mg, 0.2 mmol) and **23a** (57 mg, 0.2 mmol). The product was obtained as a white solid (55 mg, 66%), mp: 170-172 °C. ^{1}H NMR (500 MHz, $CDCl_3$) δ 7.69 (d, *J* = 1.4 Hz, 1H), 7.60 (d, *J* = 1.4 Hz, 1H), 7.49 (s, 1H), 7.46 – 7.41 (m, 2H), 6.32 (s, 1H), 3.86 (d, *J* = 5.8 Hz, 3H), 3.09 – 2.99 (m, 4H), 2.52 (d, *J* = 13.0 Hz, 2H), 2.19 – 2.10 (m, 2H). ESI-MS (*m/z*): 419 $[M+1]^+$.

4.1.9.3

4-(4-Bromo-1-methyl-1H-pyrazol-5-yl)-N-(4-(4-fluorophenyl)piperidin-4-yl)-thiophene-2-carboxamide ***24c***

Reagent: **4c** (57 mg, 0.2 mmol) and **23a** (57 mg, 0.2 mmol). The product was obtained as a white

solid (55 mg, 47%), mp: 170-172 °C. ^{1}H NMR (500 MHz, $CDCl_3$) δ 7.70 (d, *J* = 1.2 Hz, 1H), 7.60 (d, *J* = 1.2 Hz, 1H), 7.52 (s, 1H), 7.46 – 7.41 (m, 2H), 7.05 – 7.00 (m, 2H), 6.35 (s, 1H), 3.87 (s, 3H), 3.12 – 2.99 (m, 4H), 2.53 (d, *J* = 13.1 Hz, 2H), 2.20 – 2.11 (m, 2H). ^{13}C NMR (125 MHz, $CDCl_3$) δ 161.90 (d, J_{C-F} = 245.0 Hz), 161.79, 140.55, 139.21, 136.23, 131.78, 129.34, 128.73, 128.59, 127.02 (d, J_{C-F} = 7.3 Hz), 115.67 (d, J_{C-F} = 23.8 Hz), 94.00, 55.77, 40.82, 38.90, 32.10. ESI-MS (*m/z*): 463 $[M+1]^+$.

4.1.9.4

N-(4-(3,4-dichlorophenyl)piperidin-4-yl)-4-(1-methyl-1H-pyrazol-5-yl)thiophene-2-carboxamide ***24d***

Reagent: **4a** (42 mg, 0.2 mmol) and **23b** (67 mg, 0.2 mmol). The product was obtained as a white solid (44 mg, 74%), mp: 208-210 °C. ^{1}H NMR (500 MHz, $CDCl_3$) δ 7.60 (d, *J* = 1.4 Hz, 1H), 7.53 (d, *J* = 2.3 Hz, 1H), 7.49 (m, 2H), 7.42 – 7.39 (m, 1H), 7.31 (dd, *J* = 8.5, 2.3 Hz, 1H), 6.34 (d, *J* = 1.9 Hz, 1H), 6.29 (s, 1H), 3.93 (s, 3H), 3.06 (dd, *J* = 9.3, 3.4 Hz, 2H), 3.01 – 2.94 (m, 2H), 2.44 (d, *J* = 12.6 Hz, 2H), 2.10 – 2.03 (m, 2H). ESI-MS (*m/z*): 435 $[M+1]^+$. HRMS (ESI): *m/z* calcd for $(C_{20}H_{20}Cl_2N_4OS+H)^+$: 435.0808; found: 435.0818.

4.1.9.5

4-(4-Chloro-1-methyl-1H-pyrazol-5-yl)-N-(4-(4-fluorophenyl)piperidin-4-yl)-furan-2-carboxamide ***25a***

Reagent: **13a** (45 mg, 0.2 mmol) and **23a** (57 mg, 0.2 mmol). The product was obtained as an off-white solid (39 mg, 49%), mp: 144-145 °C. ^{1}H NMR (500 MHz, $CDCl_3$) δ 7.79 (s, 1H), 7.47 (s, 1H), 7.44 (dd, *J* = 8.5, 5.3 Hz, 2H), 7.26 (s, 1H), 7.03 (t, *J* = 8.6 Hz, 2H), 6.61 (s, 1H), 3.88 (s, 3H), 3.11 – 2.97 (m, 4H), 2.51 (d, *J* = 13.4 Hz, 2H), 2.12 (dd, *J* = 17.7, 7.2 Hz, 2H). ESI-MS (*m/z*): 403 $[M+1]^+$.

4.1.9.6

4-(4-Bromo-1-methyl-1H-pyrazol-5-yl)-N-(4-(4-fluorophenyl)piperidin-4-yl)-furan-2-carboxamide ***25b***

Reagent: **13c** (57 mg, 0.2 mmol) and **23a** (57 mg, 0.2 mmol). The product was obtained as an off-white solid (56 mg, 63%), mp: 193-194 °C. ^{1}H NMR (500 MHz, $CDCl_3$) δ 7.79 (s, 1H), 7.51 (s, 1H), 7.45 (dd, *J* = 8.8, 5.2 Hz, 2H), 7.24 (s, 1H), 7.04 (t, *J* = 8.7 Hz, 2H), 6.59 (s, 1H), 3.88 (s, 3H), 3.12 – 2.98 (m, 4H), 2.51 (d, *J* = 13.0 Hz, 2H), 2.17 – 2.10 (m, 2H). ESI-MS (*m/z*): 447 $[M+1]^+$.

4.1.9.7

4-(4-Bromo-1-methyl-1H-pyrazol-5-yl)-N-(4-(3,4-dichlorophenyl)piperidin-4-yl)furan-2-carboxamide ***25c***

Reagent: **13c** (57 mg, 0.2 mmol) and **23b** (67 mg, 0.2 mmol). The product was obtained as a yellow solid (73 mg, 74%), mp: 201-203 °C. ^{1}H NMR (500 MHz, $CDCl_3$) δ 7.81 (s, 1H), 7.54 (d, *J* = 2.2 Hz, 1H), 7.51 (s, 1H), 7.42 (d, *J* = 8.5 Hz, 1H), 7.32 (dd, *J* = 8.4, 2.3 Hz, 2H), 6.63 (s, 1H), 3.89 (s, 3H), 3.09 (d, *J* = 12.7 Hz, 2H), 3.01 (t, *J* = 11.3 Hz, 2H), 2.47 (d, *J* = 12.9 Hz, 2H), 2.13 – 2.05 (m, 2H). ^{13}C NMR (125 MHz, $CDCl_3$) δ 157.60, 147.67, 143.06, 139.48, 133.02, 132.13, 130.85, 130.48, 127.39, 124.73, 115.92, 115.37, 114.58, 94.11, 55.34, 40.47, 38.81, 32.11. ESI-MS (*m/z*): 497 $[M+1]^+$.

4.1.9.8

5-Chloro-4-(4-chloro-1-methyl-1H-pyrazol-5-yl)-N-(4-(4-fluorophenyl)piperidin-4-yl)furan-2-carboxamide ***25d***

Reagent: **13b** (52 mg, 0.2 mmol) and **23a** (57 mg, 0.2 mmol). The product was obtained as a white solid (52 mg, 60%), mp: 170-172 °C. ^{1}H NMR (500 MHz, $CDCl_3$) δ 7.50 (s, 1H), 7.47 – 7.42 (m, 2H), 7.13 (s, 1H), 7.07 – 7.01 (m, 2H), 6.47 (s, 1H), 3.79 (s, 3H), 3.10 (dd, *J* = 9.1, 3.6 Hz, 2H), 3.06 – 3.00 (m, 2H), 2.52 (d, *J* = 12.9 Hz, 2H), 2.19 – 2.12 (m, 2H). ^{13}C NMR (125 MHz, $CDCl_3$) δ 162.19 (d, J_{C-F} = 247.9 Hz), 156.42, 146.46, 138.40, 137.42, 129.01 (d, J_{C-F} = 9.9 Hz), 126.97, 126.90, 118.14, 115.88 (d, J_{C-F} = 21.5 Hz), 111.60 111.17, 55.79, 40.47, 38.46, 32.49. ESI-MS (*m/z*): 437 $[M+1]^+$.

4.1.9.9

5-Chloro-4-(4-chloro-1-methyl-1H-pyrazol-5-yl)-N-(4-(3,4-dichlorophenyl)-piperidin-4-yl)furan-2-carboxamide ***25e***

Reagent: **13b** (52 mg, 0.2 mmol) and **23b** (67 mg, 0.2 mmol). The product was obtained as a white solid (69 mg, 71%), mp: 130-133 °C. ^{1}H NMR (500 MHz, $CDCl_3$) δ 7.54 (s, 1H), 7.50 (s, 1H), 7.43 (d, *J* = 8.4 Hz, 1H), 7.35 – 7.28 (m, 2H), 6.92 (s, 1H), 3.80 (s, 3H), 3.38 (t, *J* = 11.1 Hz, 2H), 3.28 (t, *J* = 11.9 Hz, 2H), 2.79 (d, *J* = 13.9 Hz, 2H), 2.48 (t, *J* = 11.5 Hz, 2H). ^{13}C NMR (125 MHz, $CDCl_3$) δ 156.35, 146.53, 143.66, 138.49, 137.39, 133.00, 132.01, 130.77, 129.01, 127.45, 124.75, 118.10, 111.47, 111.14, 55.72, 40.76, 38.44, 32.87. ESI-MS (*m/z*): 489 $[M+1]^+$. HRMS (ESI): *m/z* calcd for $(C_{20}H_{18}Cl_4N_4O_2+H)^+$: 489.0227; found: 489.0239.

4.1.9.10

4-Bromo-N-(4-(3,4-dichlorophenyl)piperidin-4-yl)-5-(1-methyl-1H-pyrazol-5-yl)furan-2-carboxamide ***26a***

Reagent: **16a** (54 mg, 0.2 mmol) and **23b** (67 mg, 0.2 mmol). The product was obtained as an off-white solid (76 mg, 77%), mp: 118-120 °C. ^{1}H NMR (500 MHz, $CDCl_3$) δ 7.54 (d, *J* = 2.0 Hz, 1H), 7.50 (d, *J* = 2.2 Hz, 1H), 7.38 (d, *J* = 8.1 Hz, 1H), 7.30 – 7.26 (m, 2H), 6.82 (s, 1H), 6.78 (d, *J* = 2.0 Hz, 1H), 4.05 (s, 3H), 3.15 (d, *J* = 12.8 Hz, 2H), 3.03 (dd, *J* = 17.8, 10.1 Hz, 2H), 2.55 (d, *J* = 13.3 Hz, 2H), 2.21 – 2.12 (m, 2H). ^{13}C NMR (125 MHz, $CDCl_3$) δ 156.32, 147.15, 145.16, 143.21, 138.74, 132.74, 131.38, 130.54, 130.37, 127.47, 124.73, 119.14, 108.76, 101.66, 56.30, 41.84, 38.92, 35.05. ESI-MS (*m/z*): 497 $[M+1]^+$.

4.1.9.11

4-Bromo-5-(4-chloro-1-methyl-1H-pyrazol-5-yl)-N-(4-(3,4-dichlorophenyl)-piperidin-4-yl)furan-2-carboxamide ***26b***

Reagent: **16b** (61 mg, 0.2 mmol) and **23b** (67 mg, 0.2 mmol). The product was obtained as a white solid (74 mg, 70%), mp: 109-112 °C. ^{1}H NMR (500 MHz, $CDCl_3$) δ 7.55 (s, 1H), 7.50 (d, *J* = 2.2 Hz, 1H), 7.44 (d, *J* = 8.5 Hz, 1H), 7.33 – 7.27 (m, 2H), 6.66 (s, 1H), 3.90 (s, 3H), 3.40 – 3.30 (m, 2H), 3.20 (t, *J* = 12.6 Hz, 2H), 2.72 (d, *J* = 14.2 Hz, 2H), 2.49 (m, 2H). ESI-MS (*m/z*): 533 $[M+1]^+$. HRMS (ESI): *m/z* calcd for $(C_{20}H_{18}BrCl_3N_4O_2 + H)^+$: 532.9731; found: 532.9741.

4.1.9.12

4-Bromo-5-(4-bromo-1-methyl-1H-pyrazol-5-yl)-N-(4-(3,4-dichlorophenyl)-piperidin-4-yl)furan-2-carboxamide ***26c***

Reagent: **16c** (70 mg, 0.2 mmol) and **23b** (67 mg, 0.2 mmol). The product was obtained as a pale-yellow solid (93 mg, 81%), mp: 127-130 °C. ^{1}H NMR (500 MHz, $CDCl_3$) δ 7.58 (s, 1H), 7.50 (d, *J* = 2.1 Hz, 1H), 7.42 (d, *J* = 8.5 Hz, 1H), 7.31 – 7.27 (m, 2H), 6.72 (s, 1H), 3.91 (s, 3H), 3.28 – 3.21 (m, 2H), 3.17 – 3.09 (m, 2H), 2.63 (d, *J* = 13.9 Hz, 2H), 2.35 (t, *J* = 11.6 Hz, 2H). ESI-MS (*m/z*): 577 $[M+1]^+$. HRMS (ESI): *m/z* calcd for $(C_{20}H_{18}Br_2Cl_2N_4O_2 + H)^+$: 576.9226; found: 576.9235.

4.1.9.13

4-(4-Bromo-1-methyl-1H-pyrazol-5-yl)-N-(4-(3,4-dichlorophenyl)piperidin-4-yl)-1-methyl-1H-pyrrole-2-carboxamide ***27a***

Reagent: **13d** (57 mg, 0.2 mmol) and **23b** (67 mg, 0.2 mmol). The product was obtained as an off-white solid (48 mg, 47%), mp: 178-181 °C. ^{1}H NMR (500 MHz, $CDCl_3$) δ 7.53 (d, *J* = 2.2 Hz,

1H), 7.48 (s, 1H), 7.42 (d, *J* = 8.5 Hz, 1H), 7.30 (dd, *J* = 8.5, 2.3 Hz, 1H), 6.98 (s, 1H), 6.91 (s, 1H), 6.34 (s, 1H), 3.91 (s, 3H), 3.89 (s, 3H), 3.22 – 3.05 (m, 4H), 2.53 (m, 2H), 2.24 (m, 2H). ESI-MS (*m/z*): 510 $[M+1]^+$.

4.1.9.14

5-Bromo-4-(4-bromo-1-methyl-1H-pyrazol-5-yl)-N-(4-(3,4-dichlorophenyl)piperidin-4-yl)-1-methyl-1H-pyrrole-2-carboxamide ***27b***

Reagent: **13e** (72 mg, 0.2 mmol) and **23b** (67 mg, 0.2 mmol). The product was obtained as a yellow solid (45 mg, 38%), mp: 149-151 °C. ^{1}H NMR (500 MHz, $CDCl_3$) δ 7.53 – 7.49 (m, 2H), 7.41 (dd, *J* = 8.4, 4.2 Hz, 1H), 7.29 (dd, *J* = 8.4, 2.3 Hz, 1H), 6.88 (s, 1H), 6.43 (s, 1H), 3.90 (s, 3H), 3.77 (s, 3H), 3.15 (d, *J* = 12.7 Hz, 2H), 3.06 (dd, *J* = 22.0, 10.4 Hz, 2H), 2.51 (d, *J* = 13.4 Hz, 2H), 2.21 – 2.12 (m, 2H). ^{13}C NMR (125 MHz, $CDCl_3$) δ 160.11, 145.66, 139.06, 135.11, 132.77, 131.23, 130.57, 127.90, 127.37, 124.56, 113.55, 112.71, 110.79, 95.38, 56.12, 41.77, 38.32, 35.26, 35.07. ESI-MS (*m/z*): 590 $[M+1]^+$.

4.1.9.15

3,5-Dichloro-4-(4-chloro-1-methyl-1H-pyrazol-5-yl)-N-(4-(3,4-dichlorophenyl)piperidin-4-yl)-1-methyl-1H-pyrrole-2-carboxamide ***27c***

Reagent: **13f** (61 mg, 0.2 mmol) and **23b** (67 mg, 0.2 mmol). The product was obtained as a white solid (71 mg, 66%), mp: 131-134 °C. ^{1}H NMR (500 MHz, $CDCl_3$) δ 7.56 – 7.50 (m, 2H), 7.43 (d, *J* = 8.5 Hz, 1H), 7.31 (dd, *J* = 8.5, 2.1 Hz, 1H), 6.91 (s, 1H), 3.85 (s, 3H), 3.76 (s, 3H), 3.17 – 2.98 (m, 4H), 2.50 – 2.36 (m, 2H), 2.18 – 2.00 (m, 2H). ^{13}C NMR (125 MHz, $CDCl_3$) δ 158.35, 145.98, 137.15, 132.75, 131.06, 130.55, 129.79, 127.41, 124.56, 123.55, 122.81, 113.93, 111.99, 106.87, 56.90, 41.87, 38.11, 35.92, 34.45. ESI-MS (*m/z*): 536 $[M+1]^+$.

4.1.9.16 4-(4-Chloro-1-methyl-1H-pyrazol-5-yl)-N-(4-(3,4-dichlorophenyl)piperidin-4-yl)benzamide ***28a***

Reagent: **19a** (47 mg, 0.2 mmol) and **23b** (67 mg, 0.2 mmol). The product was obtained as a white solid (64 mg, 69%), mp: 99-102 °C. ^{1}H NMR (500 MHz, $CDCl_3$) δ 7.95 (d, *J* = 8.0 Hz, 2H), 7.51 (d, *J* = 7.8 Hz, 2H), 7.47 (d, *J* = 8.0 Hz, 2H), 7.41 – 7.35 (m, 1H), 7.30 (d, *J* = 7.3 Hz, 1H), 7.20 (s, 1H), 3.79 (s, 3H), 3.34 – 3.20 (m, 4H), 2.76 (d, *J* = 13.8 Hz, 2H), 2.36 (m, 2H). ^{13}C NMR (125 MHz, $CDCl_3$) δ 166.55, 144.62, 138.32, 137.29, 134.69, 132.84, 13158, 131.47, 130.66, 129.90, 127.69, 127.41, 124.70, 109.17, 55.87, 41.13, 38.45, 33.38. ESI-MS (*m/z*): 465 $[M+1]^+$. HRMS (ESI): *m/z*

calcd for $(C_{22}H_{21}Cl_3N_4O+H)^+$: 465.0824; found: 465.0836.

4.1.9.17 4-(4-Bromo-1-methyl-1H-pyrazol-5-yl)-N-(4-(3,4-dichlorophenyl)piperidin-4-yl)benzamide ***28b***

Reagent: **19b** (56 mg, 0.2 mmol) and **23b** (67 mg, 0.2 mmol). The product was obtained as a white solid (78 mg, 77%), mp: 148-150 °C. ^{1}H NMR (500 MHz, $CDCl_3$) δ 7.93 (d, *J* = 8.3 Hz, 2H), 7.55 (d, *J* = 2.3 Hz, 1H), 7.53 (d, *J* = 2.3 Hz, 1H), 7.50 (d, *J* = 8.3 Hz, 2H), 7.42 (d, *J* = 8.5 Hz, 1H), 7.31 (dd, *J* = 8.5, 2.3 Hz, 1H), 6.74 (s, 1H), 3.82 (s, 3H), 3.25 – 3.12 (m, 4H), 2.63 (d, *J* = 13.8 Hz, 2H), 2.32 – 2.23 (m, 2H). ^{13}C NMR (125 MHz, $CDCl_3$) δ 166.12, 145.05, 140.01, 139.45, 135.00, 132.84, 132.01, 131.43, 130.60, 130.20, 127.44, 127.42, 124.66, 93.86, 56.12, 41.23, 38.47, 34.39. ESI-MS (*m/z*): 507 $[M+1]^+$.

4.2. Pharmacological assay

4.2.1 Akt1 assay

The Akt1 inhibitory activities were determined using the homogeneous time-resolved fluorescence (HTRF) KinEASE-STK S1 kit (Cat.#62ST2PEC, Cisbio) according to the manufacturer's instructions. Akt1 kinase was expressed and purified from Escherichia coli system in-house. In short, the kinase reactions were carried out in a 384 ProxiPlate with 10 μL reaction volume per well containing 0.25 μg/mL Akt1, 1 μM peptide substrate, test compound and 20 μM ATP in assay buffer (50 mM HEPES pH 7.5, 0.01% BRIJ-35, 5 mM $MgCl_2$, 1 mM EGTA). After incubation for 1 h at r.t., the reaction was stopped by the addition of 5μL Sa-XL665 and 5 μL STK Antibody-Eu(K) in EDTA. The plate was sealed and incubated for 1 h at r.t., and the resulting TR-FRET signal was measured on Envision-PerkinElmer. The fluorescence emission was measured at 615 nm (cryptate) and 665 nm (XL665). An Emission Ratio was calculated (665/615) for each well and the Percent inhibitions were expressed as follows: Percent inhibition = (max-sample Ratio)/ (max-min)*100 ("Min" means the Ratio of no enzyme control and "max" means the Ratio of DMSO control). Compounds were initially tested at a fixed concentration (1 μg/mL), and those displaying more than 50% inhibition were further tested for dose–response IC_{50} values.

4.2.2 Kinase selectivity assay

To determine the kinase selectivity of the target compounds, the representative **25e** was assayed

against a panel of 22 protein kinases at SHANGHAI CHEMPARTNER CO.LTD. All the proteins and kinase assay kits were mainly purchased from Carna, Invitrogen or Millipore. Compound **25e** was tested at concentrations of 0.5 and 10 μM over most kinases, including ABL, ALK, Akt2, Akt3, JNK2, JAK2, ROCK1, RSK1, P70S6K, MSK1, SGK, PDK1 and PRKG1, using Mobility shift assay with ATP concentration at Km. PI3Kα inhibitory activity was screened by Kinase-Glo Luminescent Assay kit (Promege) with ATP concentration at 25μM. CHK1 and TSSK1 inhibitory activities were determined using the Luminescent ADP-Glo assay kit (Promege). In addition, the inhibition of mTOR activity was evaluated in a Lance Ultra assay. Moreover, PKA, GSK3β and CDK2/cyclin A activities were evaluated at the concentration of 1 μg/mL by Z-LYTE Kinase Assay kits (Invitrogen). Like Akt1 assay, the Aurora A and BRAF inhibitory activities of compound **25e** were measured by the HTRF Kinase Assay kits purchased from Cisbio. The protocols for these assays could be found in the manufacturer's instructions.

4.2.3 Anti-proliferative assay

All of the prepared target compounds were tested for their anti-proliferative activities *in vitro* against two human cancer cell lines including OVCAR-8 (Ovarian Adenocarcinoma) and HCT116 (Human Colon Cancer) by sulforhodamin B (SRB) assay. OVCAR-8 and HCT-116 cells were seeded into 96-well plates and cultured for 10 h. Subsequently, it was exposed to serial concentrations of compound for 72 h. Cells were then washed with PBS and fixed with 10% (w/v) trichloroacetic acid at 4 °C for 1 hour. After washing, the cells were stained for 30 min with 0.4% SRB dissolved in 1% acetic acid and then washed by 1% acetic acid for 5 times. Finally, the protein-bound dye was extracted using 10 mM unbuffered Tris base. The absorbance was obtained at 515 nm on a multiscan spectrum (Thermo Fisher). The inhibition rate on cell proliferation of each well was calculated using the formula of (A515 control cells - A515 treated cells)/A515 control cells × 100%. Data was presented in MS Excel and the curves fitted by Graphpad Prism 5.0.

4.2.4 Western blot assay

PC-3 prostate cancer cells were exposed to compound **25e** at 1uM and 10 uM for 3 h, and were then trypsinized and wash once with 2ml PBS. Protein samples were prepared by adding 100 μL RIPA lysis buffer (50 mM Tris-HCl pH 8.0, 150 mM NaCl, 1% NP-40, 0.5% sodium deoxycholate,

0.1% SDS) with protease and phosphatase inhibitor (Roche, Cat.#4693124001) onto cells and all cell lysate was collected and then centrifuged at 4˚C. The supernatant was collected as protein sample, and the total concentration was quantified using BCA kit (Pierce, Cat.#23225) and normalized. Subsequently, Proteins were transferred from gel to a nitrocellulose membrane (Life Tech, IB301002), and membrane was blocked in SuperBlock blocking buffer (Thermo Fisher, Cat. #37535) for 1 h, then in primary antibody dilution overnight at 4˚C (Rabbit anti-pAKT(S473), anti-AKT and anti-GSK3β(S9) were purchased from Cell signaling; Rabbit anti-GSK3β and mouse anti-GAPDH were purchased from Abcam). After 5×5 minutes washes in TBST buffer (25mM Tris HCL pH7.6, 150mM NaCl, 0.1% Tween-20), membrane was incubated in diluted secondary antibody for 1 h at r.t., and washed in TBST again. Membrane was imaged using LICOR Oddessy system.

4.2.5 ELISA assay

ELISA plates were prepared by coating with anti-PRAS40 antibody (R&D Systems), and blocked with 5% Milk/0.1% Tween-20. LNCaP Cells were seeded at 25,000 cells/96-well overnight and treated with DMSO or various concentrations of compounds for 1 h. Subsequently, cells were lysed in 20 mM Tris-HCl (pH 8.0), 137 mM NaCl, 2 mM EDTA, 10% glycerol and 1% Triton X-100 and lysates transferred to ELISA plates and incubated overnight. The plates were washed and incubated with rabbit anti- PRAS40 (pThr246) antibody (R&D Systems) for 1 h. After washing, plates were developed using HRP-linked anti-rabbit IgG, and 3,39,5,59-tetramethylbenzidine as substrate. Absorption was measured in a microplate spectrophotometer at 450 nm, Dose−response curves were generated using the four-parameter logistic model, and 50% inhibitory concentration (IC_{50}) values were determined from these curve fits.

4.3. Molecular docking

Docking analysis was carried out by using C-DOCKER module (Discovery Studio, version 2.5; Accelrys, San Diego, CA, USA, 2008) to compare the binding modes between compound **25e** and **28a** bound to Akt1. The X-ray crystal structure of Akt1 (PDB ID: 4GV1) was used for the docking calculation. After removing the ligand and water molecules, the CHARMm-force field was applied to the protein. And the ATP binding pocket was chosen as the active site with a radius set as 8 Å. The ligands were generated random conformations using CHARMm-based molecular dynamics (1000

steps), and then docked into the defined Akt1 binding site. The other parameters were set as default. The final binding conformation of **25e** and **28a** was determined based on the calculated CDOCKING ENERAGE. The most stable binding modes among the top 10 docking poses of **25e** and **28a** were presented in Fig. 6A and 6B, respectively.

Acknowledgement

We thank Mrs. Jianyang Pan (Pharmaceutical Informatics Institute, Zhejiang University) for performing the NMR spectrometry, the support from Zhejiang province Provincial Natural Science Foundation of China (LY13H300002) and Program for Zhejiang Leading Team of S&T Innovation (2011R50014).

Reference:

[1] P.X. Liu, H.L. Cheng, T.M. Roberts, J.J. Zhao, Targeting the phosphoinositide 3-kinase pathway in cancer, Nat. Rev. Drug Discov. 8 (2009) 627-644.
[2] B.D. Manning, L.C. Cantley, AKT/PKB signaling: navigating downstream, Cell 129 (2007) 1261-1274.
[3] C.S. Mitsiades, N. Mitsiades, M. Koutsilieris, The Akt pathway: Molecular targets for anti-cancer drug development, Curr. Cancer Drug Tar. 4 (2004) 235-256.
[4] Bellacosa, C.C. Kumar, A. Di Cristofano, J.R. Testa, Activation of AKT kinases in cancer: implications for therapeutic targeting, Adv. Cancer Res. 94 (2005) 29-86.
[5] J.Q. Cheng, B. Ruggeri, W.M. Klein, G. Sonoda, D.A. Altomare, D.K. Watson, J.R. Testa, Amplification of AKT2 in human pancreatic cancer cells and inhibition of ATK2 expression and tumorigenicity by antisense RNA, Proc. Natl. Acad. Sci. U. S. A. 93 (1996) 3636-3641.
[6] J.R. Testa, A. Bellacosa, AKT plays a central role in tumorigenesis, Proc. Natl. Acad. Sci. U. S. A. 98 (2001) 10983-10985.
[7] S.P. Staal, Molecular-Cloning of the Akt Oncogene and Its Human Homologs Akt1 and Akt2 - Amplification of Akt1 in a Primary Human Gastric Adenocarcinoma, Proc. Natl. Acad. Sci. U. S. A. 84 (1987) 5034-5037.
[8] A.S. Clark, K. West, S. Streicher, P.A. Dennis, Constitutive and inducible Akt activity promotes resistance to chemotherapy, trastuzumab, or tamoxifen in breast cancer cells, Mol. Cancer Ther. 1 (2002) 707-717.
[9] A. Lassen, M. Atefi, L. Robert, D.J. Wong, M. Cerniglia, B. Comin-Anduix, A. Ribas, Effects of AKT inhibitor therapy in response and resistance to BRAF inhibition in melanoma, Mol. Cancer 13 (2014) 83.
[10] D. Kim, H.C. Dan, S. Park, L. Yang, Q. Liu, S. Kaneko, J. Ning, L. He, H. Yang, M. Sun, S.V. Nicosia, J.Q. Cheng, AKT/PKB signaling mechanisms in cancer and chemoresistance, Front Biosci. 10 (2005) 975-987.
[11] M.E. Mattmann, S.L. Stoops, C.W. Lindsley, Inhibition of Akt with small molecules and

biologics: historical perspective and current status of the patent landscape, Expert Opin. Ther. Pat. 21 (2011) 1309-1338.
[12] S. Sestito, G. Nesi, S. Daniele, A. Martelli, M. Digiacomo, A. Borghini, D. Pietra, V. Calderone, A. Lapucci, M. Falasca, P. Parrella, A. Notarangelo, M.C. Breschi, M. Macchia, C. Martini, S. Rapposelli, Design and synthesis of 2-oxindole based multi-targeted inhibitors of PDK1/Akt signaling pathway for the treatment of glioblastoma multiforme, Eur. J. Med. Chem. 105 (2015) 274-288.
[13] S. Jangir, V. Bala, N. Lal, L. Kumar, A. Sarswat, A. Kumar, Hamidullah, K.S. Saini, V. Sharma, V. Verma, J.P. Maikhuri, R. Konwar, G. Gupta, V.L. Sharma, Novel alkylphospholipid-DTC hybrids as promising agents against endocrine related cancers acting via modulation of Akt-pathway, Eur. J. Med. Chem. 85 (2014) 638-647.
[14] S.K. Pal, K. Reckamp, H. Yu, R.A. Figlin, Akt inhibitors in clinical development for the treatment of cancer, Expert Opin. Investig. Drugs 19 (2010) 1355-1366.
[15] T. Ippolito, N. Czuczman, C. Mavis, D. Rolland, M. Lim, A. Tiwari, M.S. Cairo, R.R. Miles, M.J. Barth, MK-2206, an Akt inhibitor, decreases proliferation, induces cell cycle arrest and increases responsiveness to chemotherapy in therapy-sensitive and -resistant Burkitt lymphoma cell line models, Br. J. Haematol. 171 (2015) 25-25.
[16] H. Hirai, H. Sootome, Y. Nakatsuru, K. Miyama, S. Taguchi, K. Tsujioka, Y. Ueno, H. Hatch, P.K. Majumder, B.S. Pan, H. Kotani, MK-2206, an allosteric Akt inhibitor, enhances antitumor efficacy by standard chemotherapeutic agents or molecular targeted drugs in vitro and in vivo, Mol. Cancer Ther. 9 (2010) 1956-1967.
[17] J.F. Blake, R. Xu, J.R. Bencsik, D. Xiao, N.C. Kallan, S. Schlachter, I.S. Mitchell, K.L. Spencer, A.L. Banka, E.M. Wallace, S.L. Gloor, M. Martinson, R.D. Woessner, G.P. Vigers, B.J. Brandhuber, J. Liang, B.S. Safina, J. Li, B. Zhang, C. Chabot, S. Do, L. Lee, J. Oeh, D. Sampath, B.B. Lee, K. Lin, B.M. Liederer, N.J. Skelton, Discovery and preclinical pharmacology of a selective ATP-competitive Akt inhibitor (GDC-0068) for the treatment of human tumors, J. Med. Chem. 55 (2012) 8110-8127.
[18] M. Addie, P. Ballard, D. Buttar, C. Crafter, G. Currie, B.R. Davies, J. Debreczeni, H. Dry, P. Dudley, R. Greenwood, P.D. Johnson, J.G. Kettle, C. Lane, G. Lamont, A. Leach, R.W.A. Luke, J. Morris, D. Ogilvie, K. Page, M. Pass, S. Pearson, L. Ruston, Discovery of 4-Amino-N-[(1S)-1-(4-chlorophenyl)-3-hydroxypropyl]1-(7H-pyrrolo[2,3-d]pyrimidin-4-yl)piperidine-4-carboxamide (AZD5363), an Orally Bioavailable, Potent Inhibitor of Akt Kinases, J. Med. Chem. 56 (2013) 2059-2073.
[19] M. Dumble, M.C. Crouthamel, S.Y. Zhang, M. Schaber, D. Levy, K. Robell, Q. Liu, D.J. Figueroa, E.A. Minthorn, M.A. Seefeld, M.B. Rouse, S.K. Rabindran, D.A. Heerding, R. Kumar, Discovery of novel AKT inhibitors with enhanced anti-tumor effects in combination with the MEK inhibitor, PLoS One 9 (2014) e100880.
[20] S. Blagden, A. Hamilton, L. Mileshkin, M. Hall, T. Meniawy, S. Wong, S. Anandra, M. Buck, D. McAleer, B.A. Reedy, R.B. Noble, D.A. Smith, S.R. Morris, H. Gabra, Afuresertib (GSK2110183), an oral AKT kinase inhibitor, in combination with carboplatin and paclitaxel in recurrent ovarian cancer, Eur. J. Cancer 50 (2014) 7-7.
[21] R. Kurzrock, A. Patnaik, L. Rosenstein, S. Fu, K.P. Papadopoulos, D.A. Smith, G.S. Falchook, G. Chambers, J.L. Gauvin, A. Naing, L.S. Smith, T. Gonzalez, A.M. Tsimberidou, T.A. Mays, D.S. Cox, D.S. Hong, D.J. DeMarini, N.T. Le, S.R. Morris, A.W. Tolcher, Phase I dose-escalation of the

oral MEK1/2 inhibitor GSK1120212 (GSK212) dosed in combination with the oral AKT inhibitor GSK2141795 (GSK795), J. Clin. Oncol. 29 (2011) Abstr 3085.
[22] A. Spencer, S.S. Yoon, S.J. Harrison, S.R. Morris, D.A. Smith, R.A. Brigandi, J. Gauvin, R. Kumar, J.B. Opalinska, C. Chen, The novel AKT inhibitor afuresertib shows favorable safety, pharmacokinetics, and clinical activity in multiple myeloma, Blood 124 (2014) 2190-2195.
[23] A.W. Tolcher, A. Patnaik, K.P. Papadopoulos, D.W. Rasco, C.R. Becerra, A.J. Allred, K. Orford, G. Aktan, G. Ferron-Brady, N. Ibrahim, J. Gauvin, M. Motwani, M. Cornfeld, Phase I study of the MEK inhibitor trametinib in combination with the AKT inhibitor afuresertib in patients with solid tumors and multiple myeloma, Cancer Chemother. Pharmacol. 75 (2015) 183-189.
[24] H. Gungor, A. Saleem, R. Agarwal, S.P. Blagden, A. Michael, E.A. Stronach, M. Chen, E. Pickford, N.R. Rama, Y.L. Lewis, S.C. Carme, C. Salinas, D.A. Smith, E. Krachey, A. Santiago-Walker, R.N. Gunn, M. El-Bahrawy, S.A. Babar, S.R. Morris, H. Gabra, Pharmacokinetic (PK)/pharmacodynamic (PD) analysis of escalating repeat doses of the AKT inhibitor GSK2141795 (GSK795) in patients (pts) with ovarian cancer, J. Clin. Oncol. 29 (2011) Abstr 5046.
[25] U. Matulonis, A.A. Wright, S.A. Collins, S.M. Campos, P. Konstantinopoulos, K. MacNeill, S. Morrissey, V. Patterson, C. Whalen, J. Liu, A single arm, single stage phase II trial of trametinib (GSK1120212) and GSK2141795 in persistent or recurrent cervical cancer, J. Clin. Oncol. 33 (2015) Abstr TPS5618.
[26] A. Spencer, S.S. Yoon, S.J. Harrison, S. Morris, D. Smith, S.J. Freedman, R. Brigandi, A. Oliff, J.B. Opalinska, C. Chen, Novel AKT Inhibitor GSK2110183 Shows Favorable Safety, Pharmacokinetics, and Clinical Activity in Multiple Myeloma. Preliminary Results From a Phase I First-Time-In-Human Study, Blood 118 (2011) 808-808.
[27] Z.J. Fang, Y.N. Song, P. Zhan, Q.Z. Zhang, X.Y. Liu, Conformational restriction: an effective tactic in 'follow-on'-based drug discovery, Future Med. Chem. 6 (2014) 885-901.
[28] S. Hanessian, L. Auzzas, The Practice of Ring Constraint in Peptidomimetics Using Bicyclic and Polycyclic Amino Acids, Acc. Chem. Res. 41 (2008) 1241-1251.
[29] I.J. Kang, L.W. Wang, C.C. Lee, Y.C. Lee, Y.S. Chao, T.A. Hsu, J.H. Chern, Design, synthesis, and anti-HCV activity of thiourea compounds, Bioorg. Med. Chem. Lett. 19 (2009) 1950-1955.
[30] I.J. Kang, L.W. Wang, T.K. Yeh, C.C. Lee, Y.C. Lee, S.J. Hsu, Y.S. Wu, J.C. Wang, Y.S. Chao, A. Yueh, J.H. Chern, Synthesis, activity, and pharmacokinetic properties of a series of conformationally-restricted thiourea analogs as novel hepatitis C virus inhibitors, Bioorg. Med. Chem. 18 (2010) 6414-6421.
[31] A.E. Kummerle, M.M. Vieira, M. Schmitt, A.L.P. Miranda, C.A.M. Fraga, J.J. Bourguignon, E.J. Barreiro, Design, synthesis and analgesic properties of novel conformationally-restricted N-acylhydrazones (NAH), Bioorg. Med. Chem. Lett. 19 (2009) 4963-4966.
[32] R.K. Tiwari, K. Parang, Conformationally Constrained Peptides as Protein Tyrosine Kinase Inhibitors, Curr. Pharm. Des. 18 (2012) 2852-2866.
[33] G. Valle, W.M. Kazmierski, M. Crisma, G.M. Bonora, C. Toniolo, V.J. Hruby, Constrained Phenylalanine Analogs - Preferred Conformation Of the 1,2,3,4-Tetrahydroisoquinoline-3-Carboxylic Acid (Tic) Residue, Int. J. Pept. Protein Res. 40 (1992) 222-232.
[34] G. Saxty, S.J. Woodhead, V. Berdini, T.G. Davies, M.L. Verdonk, P.G. Wyatt, R.G. Boyle, D. Barford, R. Downham, M.D. Garrett, R.A. Carr, Identification of inhibitors of protein kinase B using fragment-based lead discovery, J. Med. Chem. 50 (2007) 2293-2296.

[35] K.M. Grimshaw, L.J. Hunter, T.A. Yap, S.P. Heaton, M.I. Walton, S.J. Woodhead, L. Fazal, M. Reule, T.G. Davies, L.C. Seavers, V. Lock, J.F. Lyons, N.T. Thompson, P. Workman, M.D. Garrett, AT7867 is a potent and oral inhibitor of AKT and p70 S6 kinase that induces pharmacodynamic changes and inhibits human tumor xenograft growth, Mol. Cancer Ther. 9 (2010) 1100-1110.

[36] K.S. Ashton, D.J. St Jean, S.F. Poon, M.R. Lee, J.G. Allen, S.W. Zhang, J.A. Lofgren, X.L. Zhang, C. Fotsch, R. Hungate, Design and synthesis of novel amide AKT1 inhibitors with selectivity over CDK2, Bioorg. Med. Chem. Lett. 21 (2011) 5191-5196.

[37] B.R. Davies, H. Greenwood, P. Dudley, C. Crafter, D.H. Yu, J. Zhang, J. Li, B. Gao, Q. Ji, J. Maynard, S.A. Ricketts, D. Cross, S. Cosulich, C.C. Chresta, K. Page, J. Yates, C. Lane, R. Watson, R. Luke, D. Ogilvie, M. Pass, Preclinical pharmacology of AZD5363, an inhibitor of AKT: pharmacodynamics, antitumor activity, and correlation of monotherapy activity with genetic background, Mol. Cancer Ther. 11 (2012) 873-887.

[38] N. Rhodes, D.A. Heerding, D.R. Duckett, D.J. Eberwein, V.B. Knick, T.J. Lansing, R.T. McConnell, T.M. Gilmer, S.Y. Zhang, K. Robell, J.A. Kahana, R.S. Geske, E.V. Kleymenova, A.E. Choudhry, Z. Lai, J.D. Leber, E.A. Minthorn, S.L. Strum, E.R. Wood, P.S. Huang, R.A. Copeland, R. Kumar, Characterization of an Akt kinase inhibitor with potent pharmacodynamic and antitumor activity, Cancer Res. 68 (2008) 2366-2374.

[39] J. Lin, D. Sampath, M.A. Nannini, B.B. Lee, M. Degtyarev, J. Oeh, H. Savage, Z. Guan, R. Hong, R. Kassees, L.B. Lee, T. Risom, S. Gross, B.M. Liederer, H. Koeppen, N.J. Skelton, J.J. Wallin, M. Belvin, E. Punnoose, L.S. Friedman, K. Lin, Targeting activated Akt with GDC-0068, a novel selective Akt inhibitor that is efficacious in multiple tumor models, Clin. Cancer Res. 19 (2013) 1760-1772.

Figures Caption:

Figure 1 Structures of representative Akt inhibitors in clinical trials.

Figure 2 A) The proposed rough binding model for GSK2141795 (or GSK2110183) with Akt1; B) Overlay of the energy-minimized conformations of GSK2141795 (pink) and **25e** (yellow).

Figure 3 The design concept based on the strutures of GSK2141795 and AT-7867.

Figure 4 Effect of Compound **25e** on levels of phosphorylated and total Akt and GSK3β in PC-3 cells.

Figure 5 Effect of compound **25e** (A), AZD5363 (B) and GSK2141795 (C) on inhibiting the phosphorylation of PRAS40 in LNCaP cell line, as a direct marker of Akt cell activity.

Figure 6 Proposed molecular binding modes of compound **25e** (A) and **28a** (B) at the ATP binding site of Akt1 (PDB ID: 4GV1). The coloring is described as follow: Gray, Akt1 kinase domain; Yellow, compound **25e**; Orange, compound **28a**; Red, oxygen atom; Blue, nitrogen atom; Light green, chlorine atom. Green dashed lines indicate hydrogen bonds, and all graphical pictures were made using Pymol.

Scheme 1 Reagents and conditions: (a) 1-methyl-5-(4,4,5,5-tetramethyl-1,3,2-dioxaborolan-2-yl) -1H-pyrazole, $Pd(PPh_3)_4$, K_2CO_3, 1,4-dioxane-H_2O, 80 °C, 6 h, 81%; (b) NBS or NCS, r.t., 3 h, 90-92% ; (c) $KMnO_4$, acetone, r.t., 3-4 h, 83-89%.

Scheme 2 Reagents and conditions: (a) 1-methyl-5-(4,4,5,5-tetramethyl-1,3,2-dioxaborolan-2-yl) -1H-pyrazole, $Pd(PPh_3)_4$, $K_3PO_4 \cdot 3H_2O$, DMF, 80-120 °C, 5–10 h, 68-95%; (b) (i) NBS or NCS, THF-DMF, r.t.–80 °C, 0.5–6 h, 70–97% ; (ii) NaOH, THF–H_2O, r.t., 3–10 h, 89–100% .

Scheme 3 The synthetic route for the target compounds **24a-d**, **25a-e**, **26a-c**, **27a-c** and **28a,b**. Reagents and conditions: (a) N,N-Bis(2-chloroethyl)benzylamine hydrochloride, tetrabutylammonium hydrogen sulfate, 50% NaOH (aq.), toluene, 85°C, 4 h, 65–70%; (b) KOH, 1,2-ethanediol, 180°C, 20 h, 71–75%; (c) diphenyl phosphoryl azide, Et_3N, anhydrous toluene, 90 °C, 3 h, then 6 N HCl, reflux, 3 h, 68–73%; (d) (i) 4a-c, 13a-f, 16a-c or 19a,b, EDCI, HOBt, TEA, DCM, 0 °C-r.t., overnight, 73-87% ; (ii) 1-chloroethyl chloroformate, 1,2-dichloroethane, r.t., 3 h, then MeOH, reflux, 1h, 87-99%.

Table 1

The AKT1 inhibitory and *in vitro* anti-proliferative activities of compounds **24a-d**, **25a-e**, **26a-c**, **27a-c** and **28a,b**.

Compd.	Akt1inhibitory activity IC_{50}[a], μM (inhibition, %)[b]	Anti-proliferative activity (IC_{50}, μM)	
		OVCAR-8	HCT116
24a	0.92	14.30	24.82
24b	0.32	8.19	18.26
24c	0.36	7.78	17.52
24d	0.071	1.61	3.92
25a	0.92	6.46	10.08
25b	2.02	20.14	18.11
25c	0.44	3.77	4.00
25d	0.39	4.81	6.47
25e	0.061	9.76	7.76
26a	(49.4%) [b]	6.87	24.77
26b	1.48	5.95	6.97
26c	(43.5%) [b]	5.81	16.40
27a	1.26	2.83	12.87
27b	(30.3%) [b]	4.70	7.75
27c	0.85	1.77	9.28
28a	1.91	5.21	11.88
28b	1.40	1.96	11.03
AZD5363	0.034	7.27	5.20
GSK2141795	0.018	/	/

[a] All IC_{50} data are the mean of three experiments.

[b] The inhibition rate of Akt1 activities were determined at a concentration of 1 μg/mL.

Table 2

Kinase selectivity profile of **25e** in comparison with that of Staurosporine

Kinase family	Kinases	% inhibition		Staurosporine
		10 μM	0.5 μM	($IC_{50,}$ nM)
AGC	**Akt1**	98.2 [a]		17.6
	Akt2	/	98.6	16
	Akt3	/	99.1	10
	PKA	90.6 [a]		8.2
	RSK1	/	88.5	1.2
	P70S6K	/	83.5	1.0
	ROCK1	/	94.4	0.68
TK	**PDK1**	24.9	3.7	5.2
	SGK	69.2	64.7	14
	MSK1	98.3	88.8	1.4
	PRKG1	87.9	85.6	5.0
	TSSK1	38.5	-3.9	0.33
	ABL	9.6	-3.0	339
	JAK2	/	-4.7	0.31
TKL	**BRAF**	7.2 [a]		5.03
	ALK	65.9	20.8	7.1
CAMK	**CHK1**	50.7	1.3	1.2
Atypical	**PI3Kα**	17.8	2.2	8.7[b]
	mTOR	13.8	/	8.8[b]
CMGC	**JNK2**	55.8	12.7	2270
	CDK2/cyclin A	5.1 [a]		5.8
	GSK3β	6.6 [a]		51.6
Other	**Aurora A**	0.43 [a]		7.63

[a] The inhibition rate was determined at a concentration of 1 μg/mL.

[b] IC_{50} value was determined used PI103 as control.

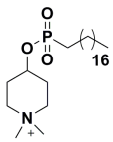

Perifosine

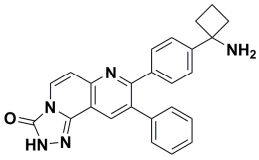

MK-2206

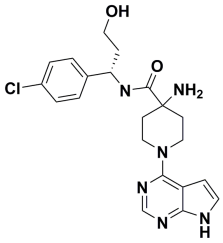

AZD5363

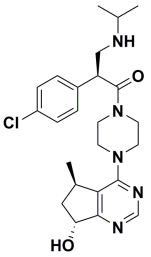

GDC-0068

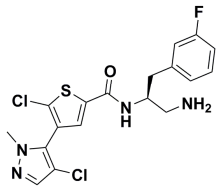

GSK2110183

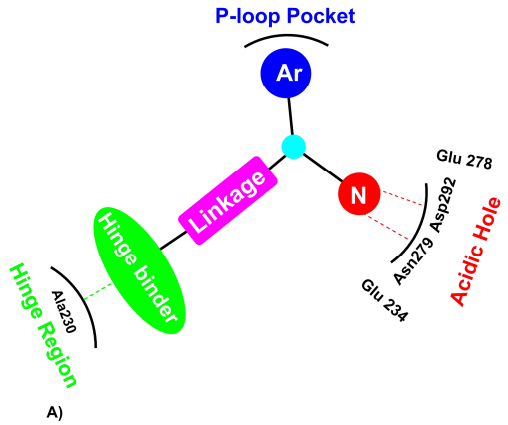

A)

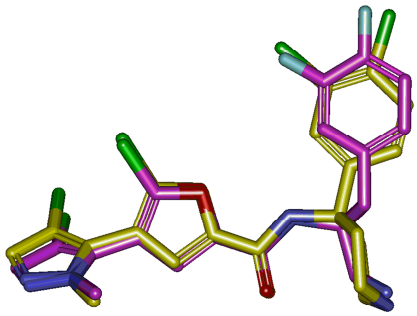

B)

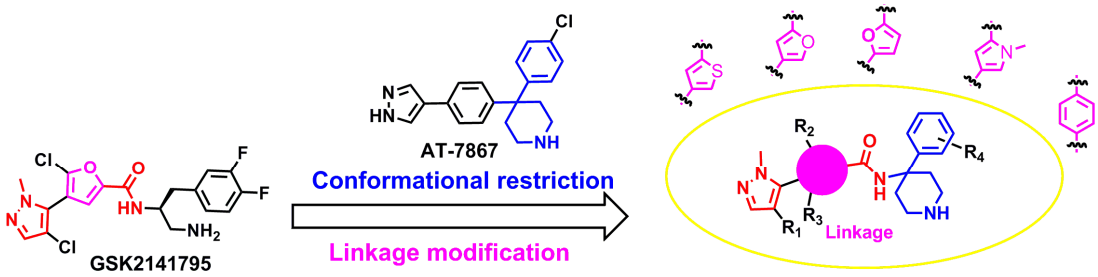

Enzyme Akt1 IC_{50} : up to 60 nM
LNCap pPRAS40 IC50: up to 30 nM

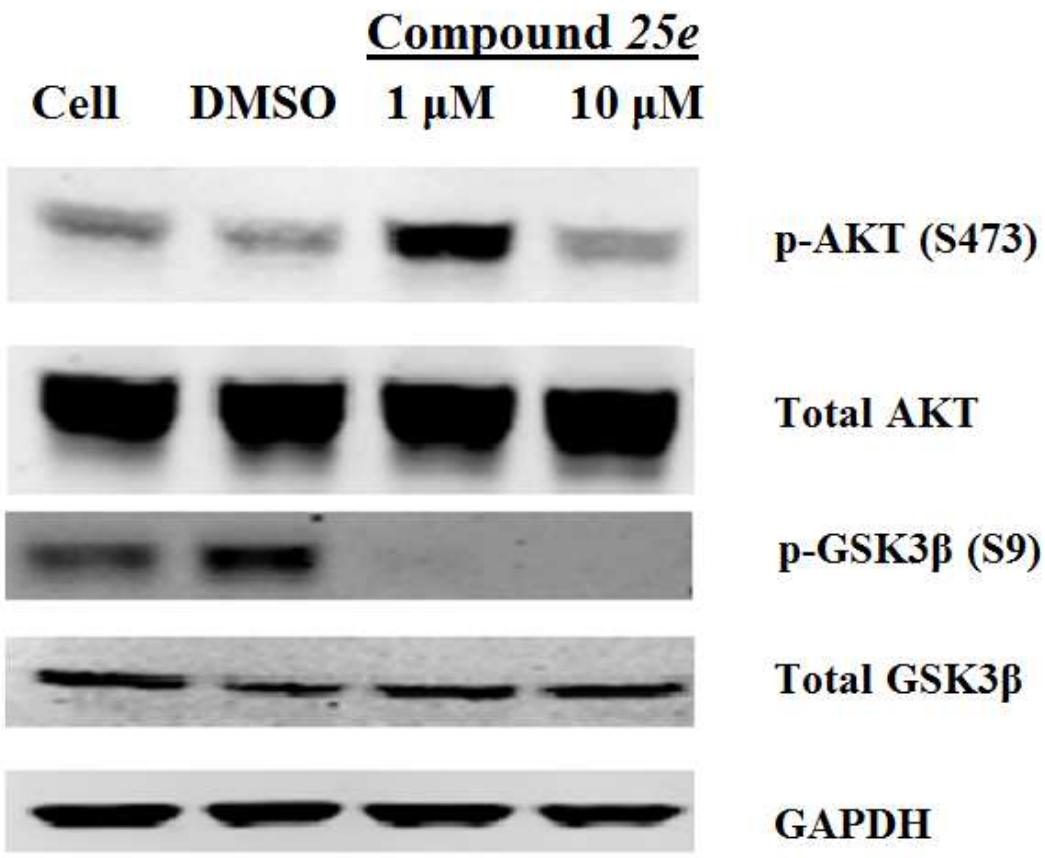

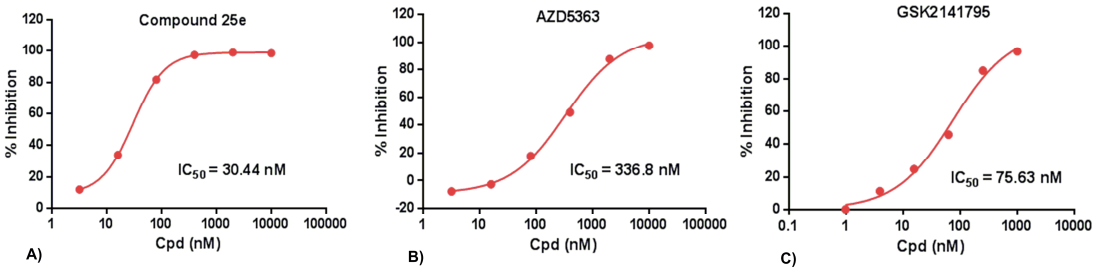

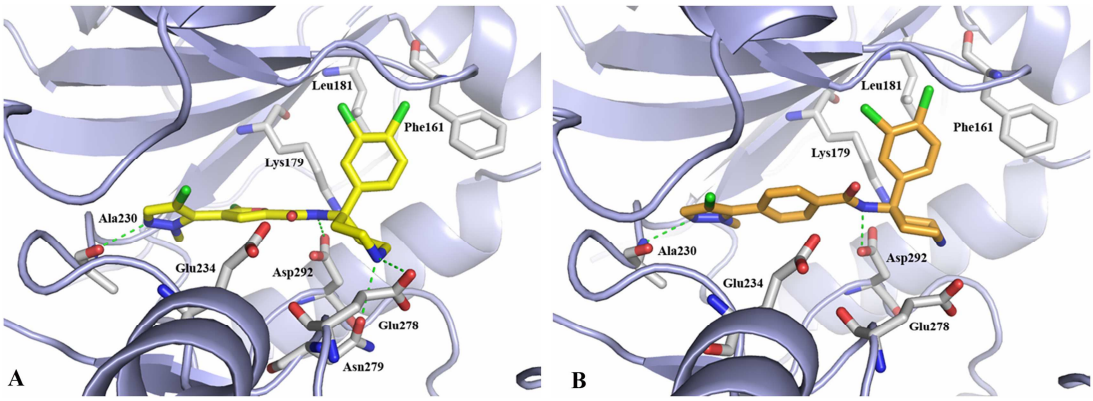

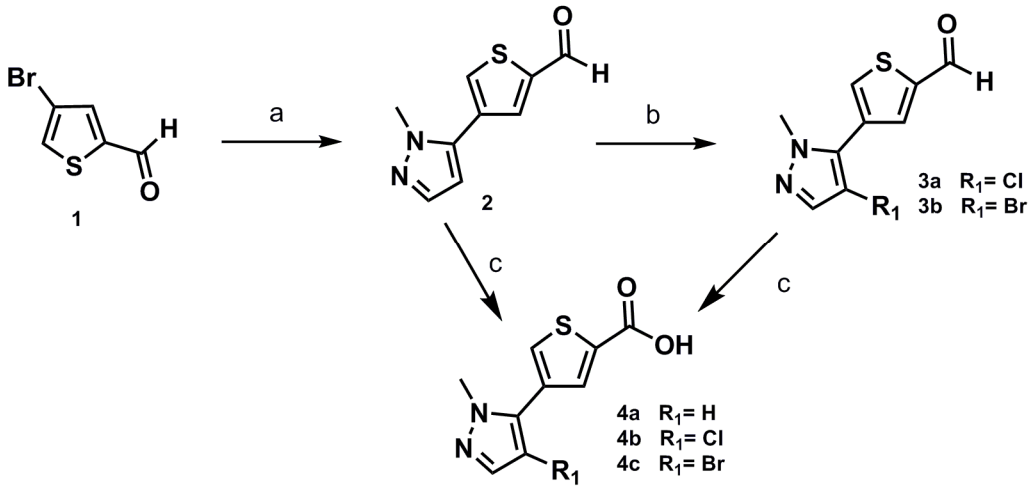

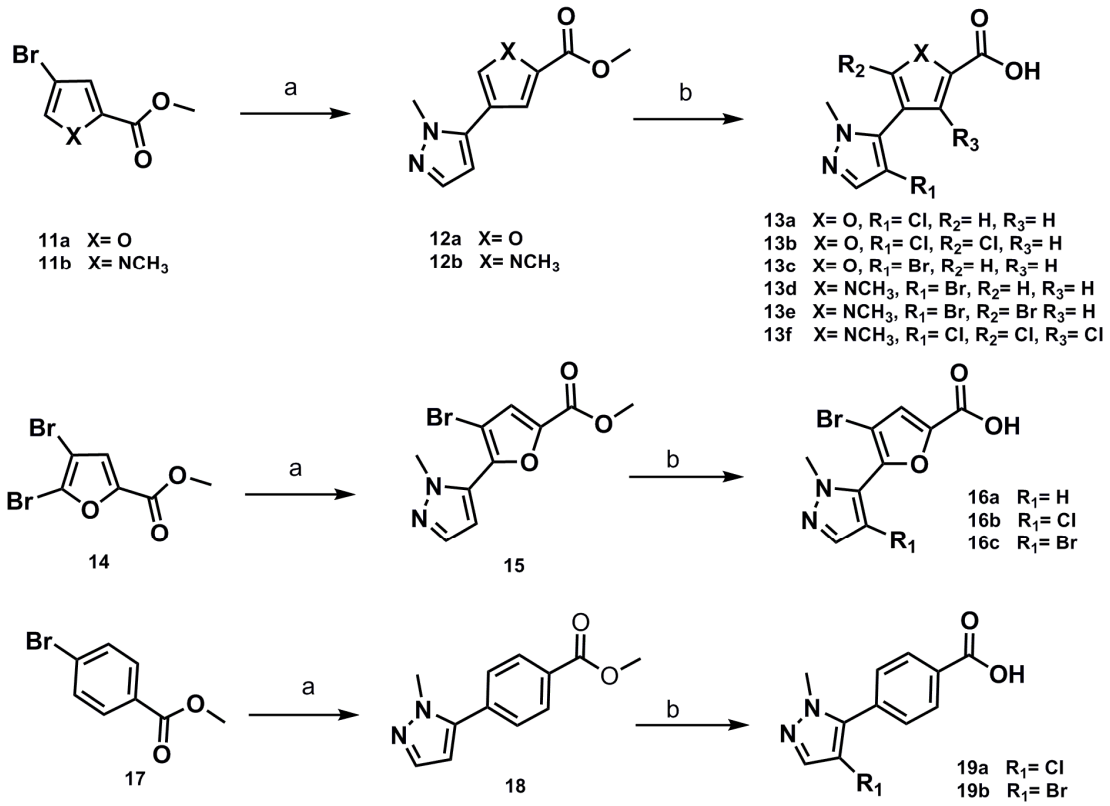

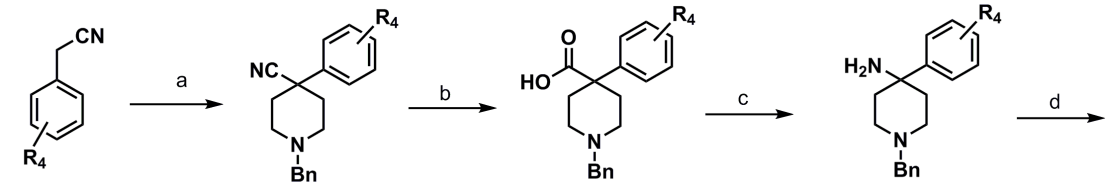

20a R_4= 4-F
20b R_4= 3,4-diCl

21a R_4= 4-F
21b R_4= 3,4-diCl

22a R_4= 4-F
22b R_4= 3,4-diCl

23a R_4= 4-F
23b R_4= 3,4-diCl

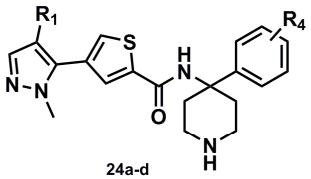

24a-d

24a R_1= H, R_4= 4-F
24b R_1= Cl, R_4= 4-F
24c R_1= Br, R_4= 4-F
24d R_1= H, R_4= 3,4-diCl

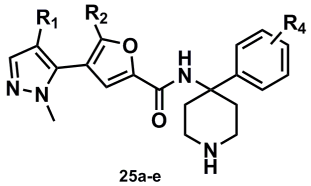

25a-e

25a R_1= Cl, R_2= H, R_4= 4-F
25b R_1= Br, R_2= H, R_4= 4-F
25c R_1= Br, R_2= H, R_4= 3,4-diCl
25d R_1= Cl, R_2= Cl, R_4= 4-F
25e R_1= Cl, R_2= Cl, R_4= 3,4-diCl

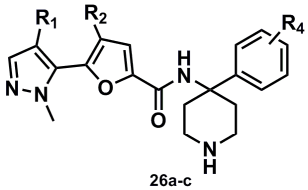

26a-c

26a R_1= H, R_2= Br, R_4= 3,4-diCl
26b R_1= Cl, R_2= Br, R_4= 3,4-diCl
26c R_1= Br, R_2= Br, R_4= 3,4-diCl

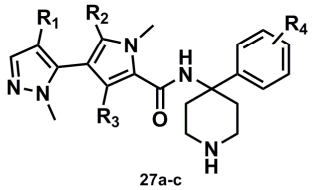

27a-c

27a R_1= Br, R_2= H, R_3= H, R_4= 3,4-diCl
27b R_1= Br, R_2= Br R_3= H, R_4= 3,4-diCl
27c R_1= Cl, R_2= Cl, R_3= Cl, R_4= 3,4-diCl

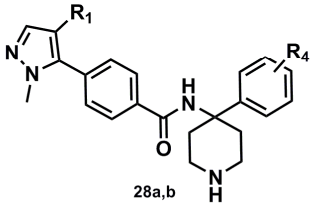

28a,b

28a R_1= Cl, R_4= 3,4-diCl
28b R_1= Br, R_4= 3,4-diCl

Highlights:

> A series of novel pyrazol-furan carboxamide analogues were designed, synthesized.

> Most compounds exhibited moderate to excellent Akt1 inhibitory activities, as well as favorable cytotoxicities.

> Kinase selectivity profile of the representative **25e** was investigated.

> **25e** significantly decreased the level of p-PRAS40 with IC_{50} value of 30.4 nM in LNCaP cell.